Synchronous Current-Mode with Constant On-Time, PWM Buck Controller

ADP1882/ADP1883

FEATURES

- Power input voltage as low as 2.75 V to 20 V
- Bias supply voltage range: 2.75 V to 5.5 V
- Minimum output voltage: 0.8 V
- 0.8 V reference voltage with ±1.0% accuracy
- Supports all N-channel MOSFET power stages
- Available in 300 kHz, 600 kHz, and 1.0 MHz options
- No current-sense resistor required
- Power saving mode (PSM) for light loads (ADP1883 only)
- Resistor-programmable current-sense gain
- Thermal overload protection
- Short-circuit protection
- Precision enable input
- Integrated bootstrap diode for high-side drive
- 140 µA shutdown supply current
- Starts into a precharged load
- Small, 10-lead MSOP package

APPLICATIONS

- Telecom and networking systems
- Mid to high end servers
- Set-top boxes
- DSP core power supplies

TYPICAL APPLICATIONS CIRCUIT

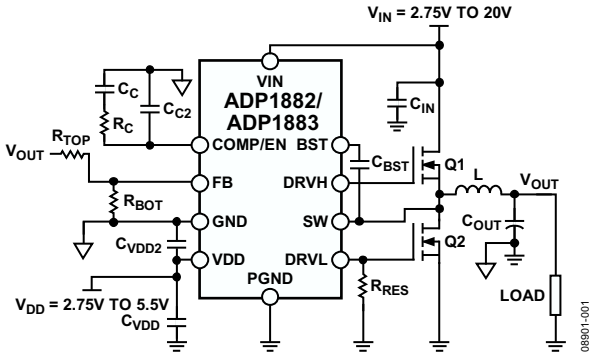

Figure 1.

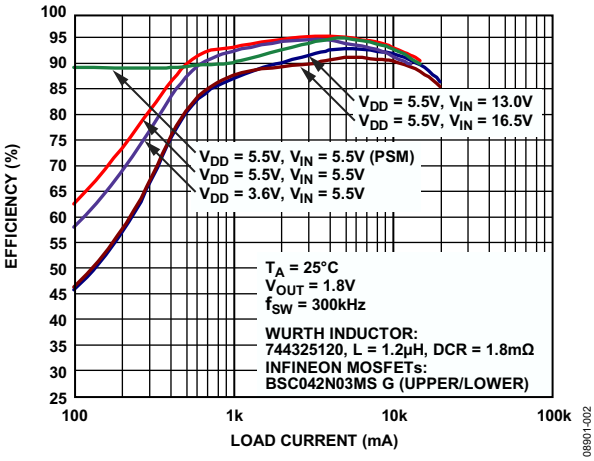

Figure 2. ADP1882/ADP1883 Efficiency vs. Load Current (V_{OUT} = 1.8 V, 300 kHz)

GENERAL DESCRIPTION

The ADP1882/ADP1883 are versatile current-mode, synchronous step-down controllers that provide superior transient response, optimal stability, and current-limit protection by using a constant on-time, pseudo-fixed frequency with a programmable current-limit, current-control scheme. In addition, these devices offer optimum performance at low duty cycles by using valley current-mode control architecture. This allows the ADP1882/ADP1883 to drive all N-channel power stages to regulate output voltages as low as 0.8 V.

The ADP1883 is the power saving mode (PSM) version of the device and is capable of pulse skipping to maintain output regulation while achieving improved system efficiency at light loads (see the Power Saving Mode (PSM) Version (ADP1883) section for more information).

Available in three frequency options (300 kHz, 600 kHz, and 1.0 MHz, plus the PSM option), the ADP1882/ADP1883 are well suited for a wide range of applications. These ICs not only operate from a 2.75 V to 5.5 V bias supply, but they also can accept a power input as high as 20 V.

In addition, an internally fixed soft start period is included to limit input in-rush current from the input supply during startup and to provide reverse current protection during soft start for a pre-charged output. The low-side current-sense, current-gain scheme and integration of a boost diode, along with the PSM/forced pulse-width modulation (PWM) option, reduce the external part count and improve efficiency.

The ADP1882/ADP1883 operate over the −40°C to +125°C junction temperature range and are available in a 10-lead MSOP.

Rev. 0

One Technology Way, P.O. Box 9106, Norwood, MA 02062-9106, U.S.A.
Tel: 781.329.4700 **www.analog.com**
Fax: 781.461.3113

TABLE OF CONTENTS

REVISION HISTORY

4/10—Revision 0: Initial Version

SPECIFICATIONS

All limits at temperature extremes are guaranteed via correlation using standard statistical quality control (SQC). V_{DD} = 5 V, BST − SW = 5 V, V_{IN} = 13 V. The specifications are valid for T_J = −40°C to +125°C, unless otherwise specified.

Table 1.

Parameter	Symbol	Conditions	Min	Typ	Max	Unit
POWER SUPPLY CHARACTERISTICS						
High Input Voltage Range	V_{IN}	ADP1882ARMZ-0.3/ADP1883ARMZ-0.3 (300 kHz)	2.75	12	20	V
		ADP1882ARMZ-0.6/ADP1883ARMZ-0.6 (600 kHz)	2.75	12	20	V
		ADP1882ARMZ-1.0/ADP1883ARMZ-1.0 (1.0 MHz)	3.0	12	20	V
Low Input Voltage Range	V_{DD}	C_{IN} = 1 µF to PGND, C_{IN} = 0.22 µF to GND				
		ADP1882ARMZ-0.3/ADP1883ARMZ-0.3 (300 kHz)	2.75	5	5.5	V
		ADP1882ARMZ-0.6/ADP1883ARMZ-0.6 (600 kHz)	2.75	5	5.5	V
		ADP1882ARMZ-1.0/ADP1883ARMZ-1.0 (1.0 MHz)	3.0	5	5.5	V
Quiescent Current	$I_{Q\_DD} + I_{Q\_BST}$	FB = 1.5 V, no switching		1.1		mA
Shutdown Current	$I_{DD,SD} + I_{BST,SD}$	COMP/EN < 285 mV		140	215	µA
Undervoltage Lockout	UVLO	Rising V_{DD} (see Figure 35 for temperature variation)		2.65		V
UVLO Hysteresis		Falling V_{DD} from operational state		190		mV
SOFT START						
Soft Start Period		See Figure 58		3.0		ms
ERROR AMPLIFIER						
FB Regulation Voltage	V_{FB}	T_J = 25°C		800		mV
		T_J = −40°C to +85°C	795.3	800	805.5	mV
		T_J = −40°C to +125°C	792.8	800	808.0	mV
Transconductance	G_M		300	520	730	µs
FB Input Leakage Current	$I_{FB,LEAK}$	FB = 0.8 V, COMP/EN = released		1	50	nA
CURRENT-SENSE AMPLIFIER GAIN						
Programming Resistor (RES) Value from DRVL to PGND		RES = 47 kΩ ± 1%	2.98	3.4	3.7	V/V
		RES = 22 kΩ ± 1%	6	6.6	7.4	V/V
		RES = none	24.1	26.7	29.3	V/V
		RES = 100 kΩ ± 1%	12.1	13.4	14.7	V/V
SWITCHING FREQUENCY		Typical values measured at 50% time points with 0 nF at DRVH and DRVL; maximum values are guaranteed by bench evaluation[1]				
ADP1882ARMZ-0.3/ ADP1883ARMZ-0.3 (300 kHz)				300		kHz
On Time		V_{IN} = 5 V, V_{OUT} = 2 V, T_J = 25°C	1115	1200	1285	ns
Minimum On Time		V_{IN} = 20 V		145	190	ns
Minimum Off Time		84% duty cycle (maximum)		340	400	ns
ADP1882ARMZ-0.6/ ADP1883ARMZ-0.6 (600 kHz)				600		kHz
On Time		V_{IN} = 5 V, V_{OUT} = 2 V, T_J = 25°C	490	540	585	ns
Minimum On Time		V_{IN} = 20 V, V_{OUT} = 0.8 V		82	110	ns
Minimum Off Time		65% duty cycle (maximum)		340	400	ns
ADP1882ARMZ-1.0/ ADP1883ARMZ-1.0 (1.0 MHz)				1.0		MHz
On Time		V_{IN} = 5 V, V_{OUT} = 2 V, T_J = 25°C	280	312	340	ns
Minimum On Time		V_{IN} = 20 V		60	85	ns
Minimum Off Time		45% duty cycle (maximum)		340	400	ns

Parameter	Symbol	Conditions	Min	Typ	Max	Unit
OUTPUT DRIVER CHARACTERISTICS						
High-Side Driver						
Output Source Resistance		I_{SOURCE} = 1.5 A, 100 ns, positive pulse (0 V to 5 V)		2	3.5	Ω
Output Sink Resistance		I_{SINK} = 1.5 A, 100 ns, negative pulse (5 V to 0 V)		0.8	2	Ω
Rise Time[2]	$t_{R, DRVH}$	BST − SW = 4.4 V, C_{IN} = 4.3 nF (see Figure 60)		25		ns
Fall Time[2]	$t_{F, DRVH}$	BST − SW = 4.4 V, C_{IN} = 4.3 nF (see Figure 61)		11		ns
Low-Side Driver						
Output Source Resistance		I_{SOURCE} = 1.5 A, 100 ns, positive pulse (0 V to 5 V)		1.7	3	Ω
Output Sink Resistance		I_{SINK} = 1.5 A, 100 ns, negative pulse (5 V to 0 V)		0.75	2	Ω
Rise Time[2]	$t_{R, DRVL}$	V_{DD} = 5.0 V, C_{IN} = 4.3 nF (see Figure 61)		18		ns
Fall Time[2]	$t_{F, DRVL}$	V_{DD} = 5.0 V, C_{IN} = 4.3 nF (see Figure 60)		16		ns
Propagation Delays						
DRVL Fall to DRVH Rise[2]	$t_{TPDH, DRVH}$	BST − SW = 4.4 V (see Figure 60)		22		ns
DRVH Fall to DRVL Rise[2]	$t_{TPDH, DRVL}$	BST − SW = 4.4 V (see Figure 61)		24		ns
SW Leakage Current	$I_{SW, LEAK}$	BST = 25 V, SW = 20 V, VDD = 5.5 V			110	µA
Integrated Rectifier						
Channel Impedance		I_{SINK} = 10 mA		22		Ω
PRECISION ENABLE THRESHOLD						
Logic High Level		V_{IN} = 2.75 V to 20 V, V_{DD} = 2.75 V to 5.5 V	235	285	330	mV
Enable Hysteresis		V_{IN} = 2.75 V to 20 V, V_{DD} = 2.75 V to 5.5 V		35		mV
COMP VOLTAGE						
COMP Clamp Low Voltage	$V_{COMP(LOW)}$	From disable state, release COMP/EN pin to enable device; 2.75 V ≤ V_{DD} ≤ 5.5 V	0.47			V
COMP Clamp High Voltage	$V_{COMP(HIGH)}$	2.75 V ≤ V_{DD} ≤ 5.5 V			2.55	V
COMP Zero Current Threshold	V_{COMP_ZCT}	2.75 V ≤ V_{DD} ≤ 5.5 V		0.95		V
THERMAL SHUTDOWN	T_{TMSD}					
Thermal Shutdown Threshold		Rising temperature		155		°C
Thermal Shutdown Hysteresis				15		°C
Hiccup Current Limit Timing				6		ms

[1] The maximum specified values are with the closed loop measured at 10% to 90% time points (see Figure 60 and Figure 61), C_{GATE} = 4.3 nF, and the upper-side and lower-side MOSFETs specified as Infineon BSC042N030MSG.
[2] Not automatic test equipment (ATE) tested.

ABSOLUTE MAXIMUM RATINGS

Table 2.

Parameter	Rating
VDD to GND	−0.3 V to +6 V
VIN to PGND	−0.3 V to +28 V
FB, COMP/EN to GND	−0.3 V to (VDD + 0.3 V)
DRVL to PGND	−0.3 V to (VDD + 0.3 V)
SW to PGND	−2.0 V to +28 V
BST to SW	−0.8 V to (VDD + 0.3 V)
BST to PGND	−0.3 V to 28 V
DRVH to SW	−0.3 V to VDD
PGND to GND	±0.3 V
θ_{JA} (10-Lead MSOP)	
2-Layer Board	213.1°C/W
4-Layer Board	171.7°C/W
Operating Junction Temperature Range	−40°C to +125°C
Storage Temperature Range	−65°C to +150°C
Soldering Conditions	JEDEC J-STD-020
Maximum Soldering Lead Temperature (10 sec)	300°C

Stresses above those listed under Absolute Maximum Ratings may cause permanent damage to the device. This is a stress rating only; functional operation of the device at these or any other conditions above those indicated in the operational section of this specification is not implied. Exposure to absolute maximum rating conditions for extended periods may affect device reliability.

Absolute maximum ratings apply individually only, not in combination. Unless otherwise specified, all other voltages are referenced to PGND.

THERMAL RESISTANCE

θ_{JA} is specified for the worst-case conditions, that is, a device soldered in a circuit board for surface-mount packages.

Table 3. Thermal Resistance

Package Type	θ_{JA}[1]	Unit
θ_{JA} (10-Lead MSOP)		
2-Layer Board	213.1	°C/W
4-Layer Board	171.7	°C/W

[1] θ_{JA} is specified for the worst-case conditions; that is, θ_{JA} is specified for device soldered in a circuit board for surface-mount packages.

BOUNDARY CONDITION

In determining the values given in Table 2 and Table 3, natural convection was used to transfer heat to a 4-layer evaluation board.

ESD CAUTION

ESD (electrostatic discharge) sensitive device. Charged devices and circuit boards can discharge without detection. Although this product features patented or proprietary protection circuitry, damage may occur on devices subjected to high energy ESD. Therefore, proper ESD precautions should be taken to avoid performance degradation or loss of functionality.

PIN CONFIGURATION AND FUNCTION DESCRIPTIONS

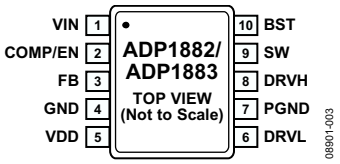

Figure 3. Pin Configuration

Table 4. Pin Function Descriptions

Pin No.	Mnemonic	Description
1	VIN	High Input Voltage. Connect VIN to the drain of the upper-side MOSFET.
2	COMP/EN	Output of the Internal Error Amplifier/IC Enable. When this pin functions as EN, applying 0 V to this pin disables the IC.
3	FB	Noninverting Input of the Internal Error Amplifier. This is the node where the feedback resistor is connected.
4	GND	Analog Ground Reference Pin of the IC. All sensitive analog components should be connected to this ground plane (see the Layout Considerations section).
5	VDD	Bias Voltage Supply for the ADP1882/ADP1883 Controller, Including the Output Gate Drivers. A bypass capacitor of 1 µF directly from this pin to PGND and a 0.1 µF across VDD and GND are recommended.
6	DRVL	Drive Output for the External Lower-Side N-Channel MOSFET. This pin also serves as the current-sense gain setting pin (see Figure 69).
7	PGND	Power GND. Ground for the lower-side gate driver and lower-side N-channel MOSFET.
8	DRVH	Drive Output for the External Upper-Side, N-Channel MOSFET.
9	SW	Switch Node Connection.
10	BST	Bootstrap for the Upper-Side MOSFET Gate Drive Circuitry. An internal boot rectifier (diode) is connected between VDD and BST. A capacitor from BST to SW is required. An external Schottky diode can also be connected between VDD and BST for increased gate drive capability.

TYPICAL PERFORMANCE CHARACTERISTICS

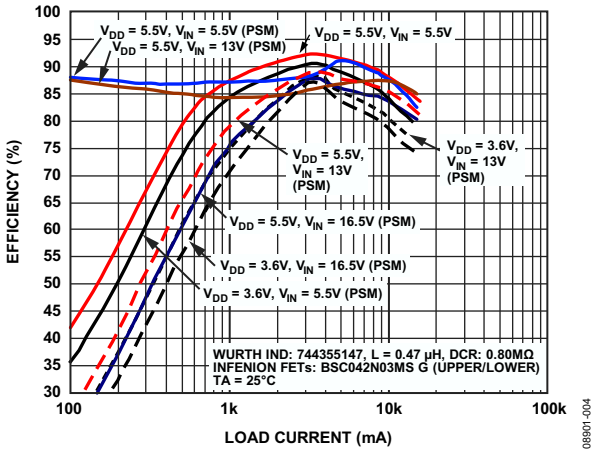

Figure 4. Efficiency—300 kHz, V_{OUT} = 0.8 V

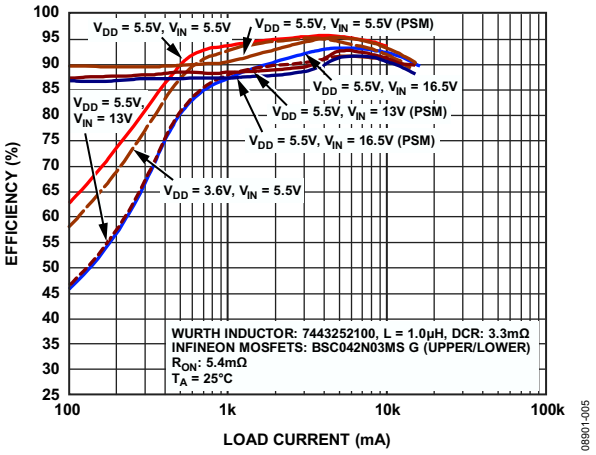

Figure 5. Efficiency—300 kHz, V_{OUT} = 1.8 V

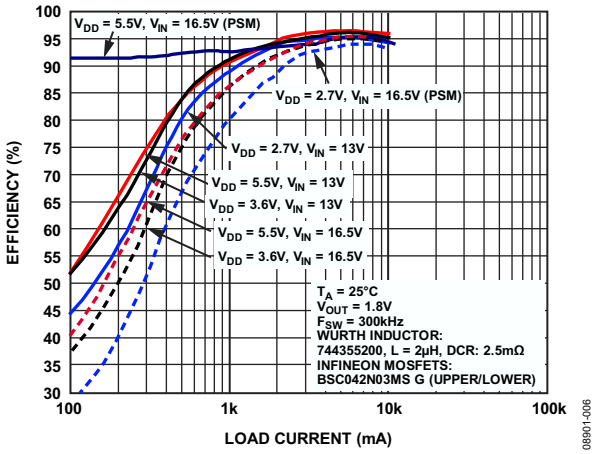

Figure 6. Efficiency—300 kHz, V_{OUT} = 7 V

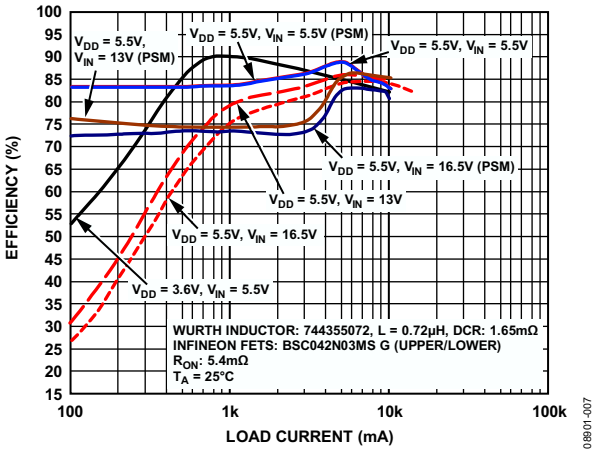

Figure 7. Efficiency—600 kHz, V_{OUT} = 0.8 V

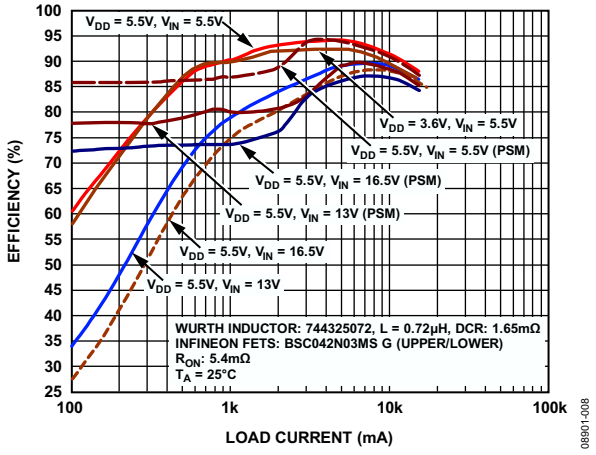

Figure 8. Efficiency—600 kHz, V_{OUT} = 1.8 V

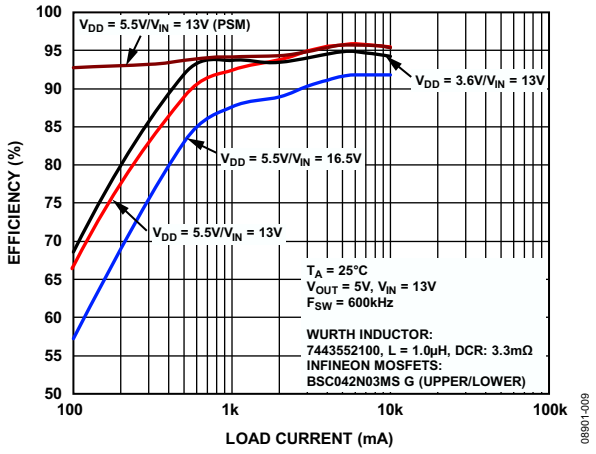

Figure 9. Efficiency—600 kHz, V_{OUT} = 5 V

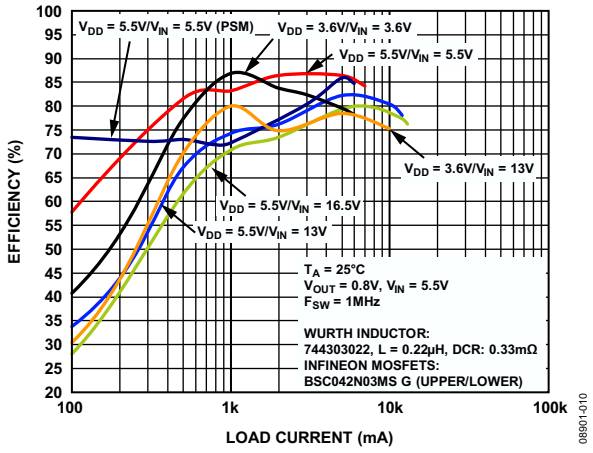

Figure 10. Efficiency—1.0 MHz, V_{OUT} = 0.8 V

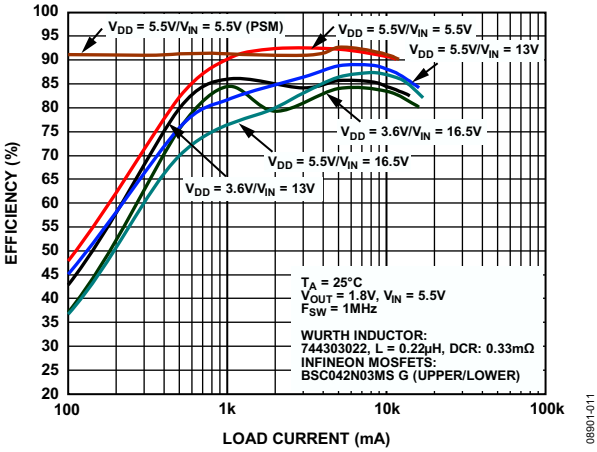

Figure 11. Efficiency—1.0 MHz, V_{OUT} = 1.8 V

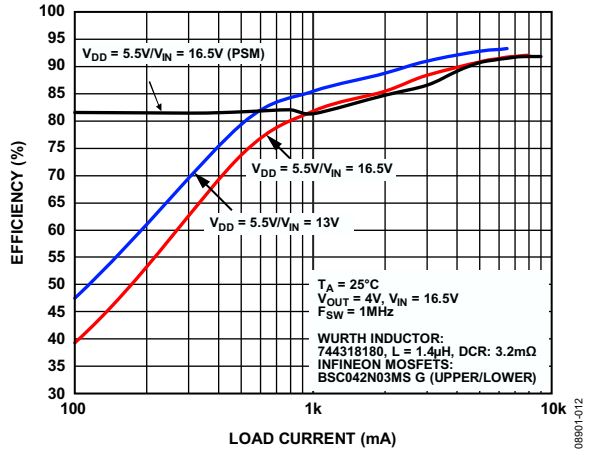

Figure 12. Efficiency—1.0 MHz, V_{OUT} = 4 V

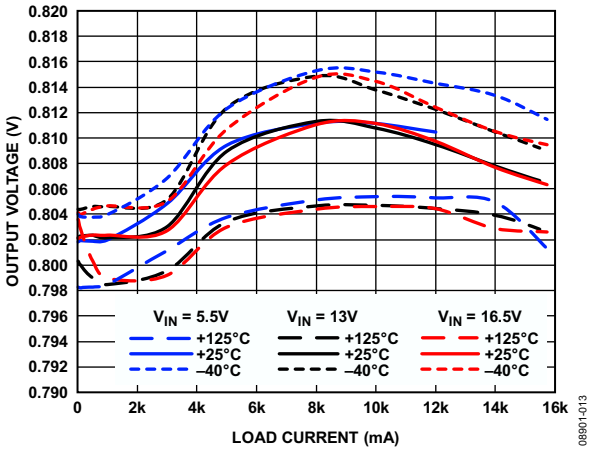

Figure 13. Output Voltage Accuracy—300 kHz, V_{OUT} = 0.8 V

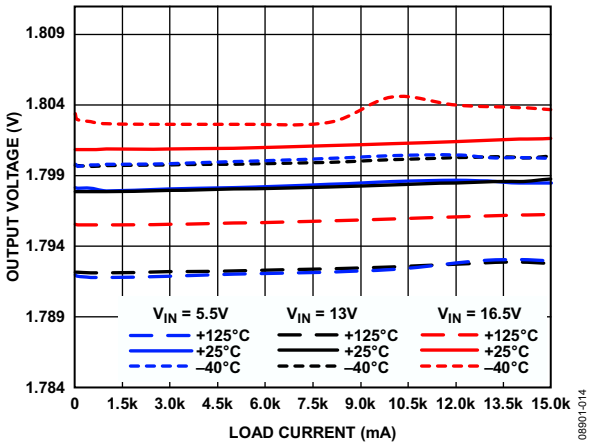

Figure 14. Output Voltage Accuracy—300 kHz, V_{OUT} = 1.8 V

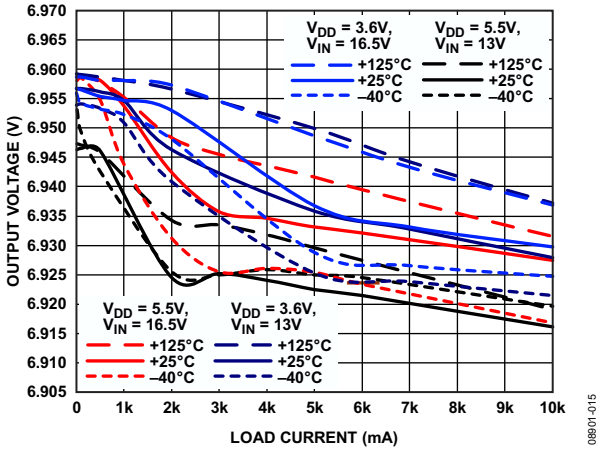

Figure 15. Output Voltage Accuracy—300 kHz, V_{OUT} = 7 V

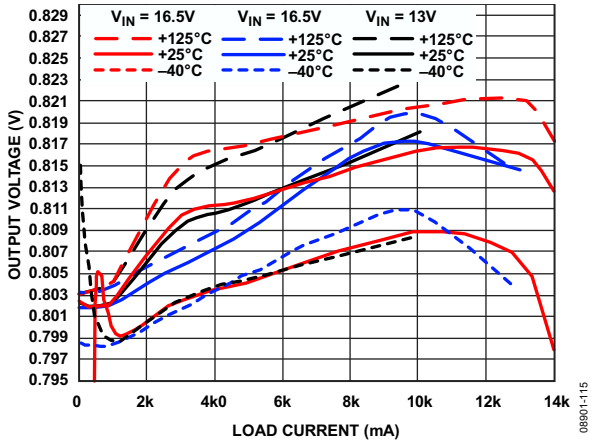

Figure 16. Output Voltage Accuracy—600 kHz, V_{OUT} = 0.8 V

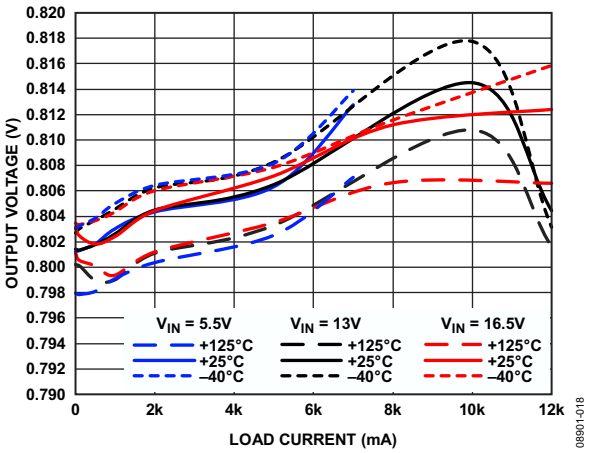

Figure 19. Output Voltage Accuracy—1.0 MHz, V_{OUT} = 0.8 V

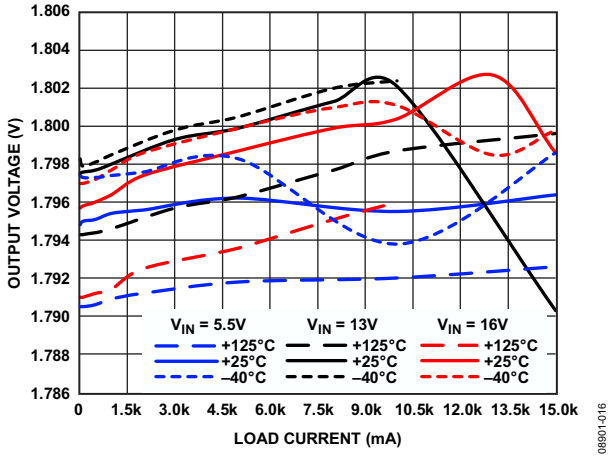

Figure 17. Output Voltage Accuracy—600 kHz, V_{OUT} = 1.8 V

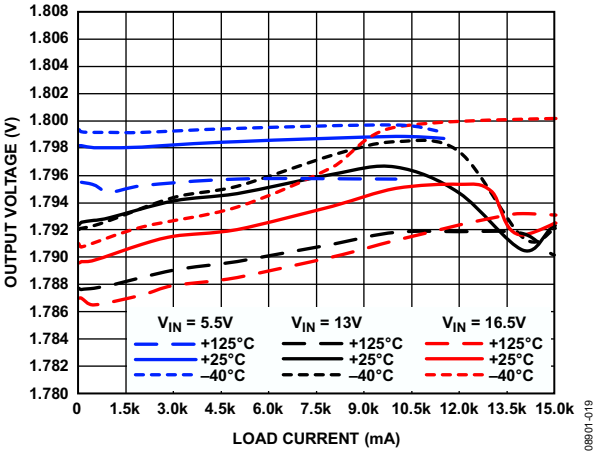

Figure 20. Output Voltage Accuracy—1.0 MHz, V_{OUT} = 1.8 V

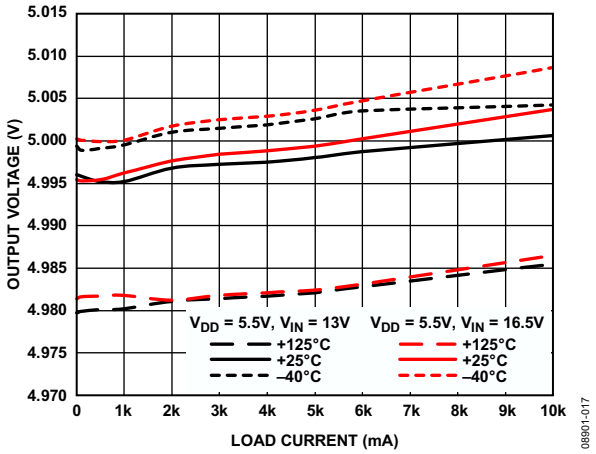

Figure 18. Output Voltage Accuracy—600 kHz, V_{OUT} = 5 V

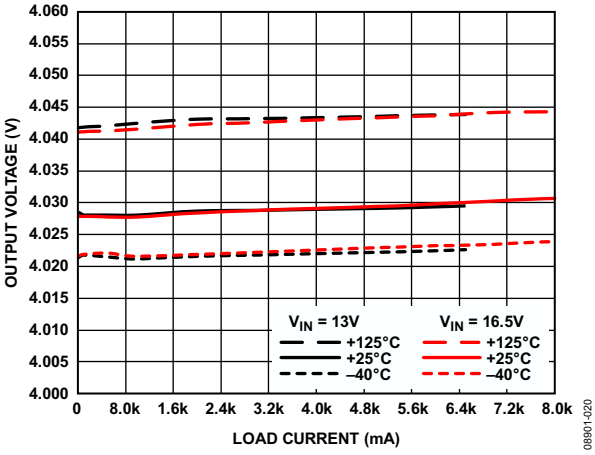

Figure 21. Output Voltage Accuracy—1.0 MHz, V_{OUT} = 4 V

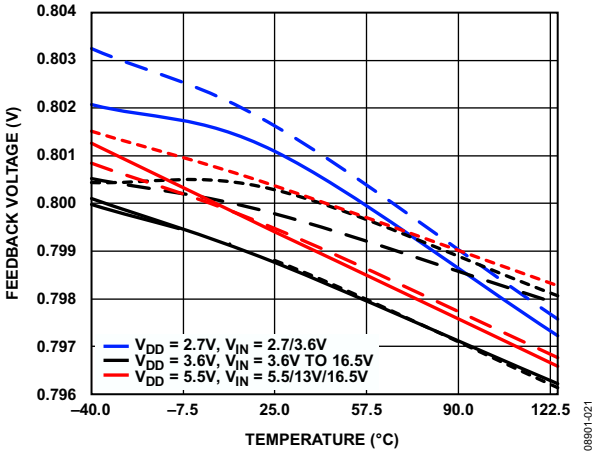

Figure 22. Feedback Voltage vs. Temperature

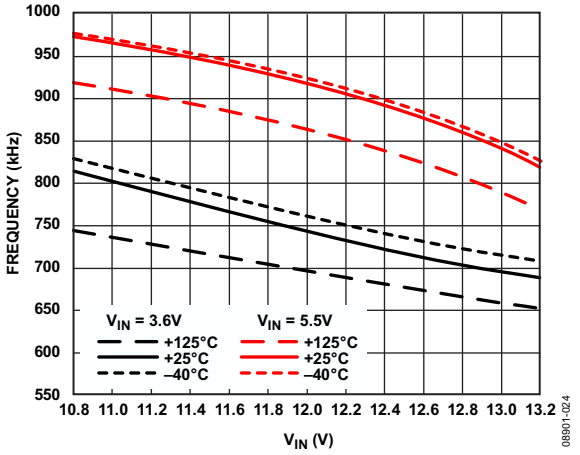

Figure 25. Switching Frequency vs. High Input Voltage, 1.0 MHz, ±10% of 12 V

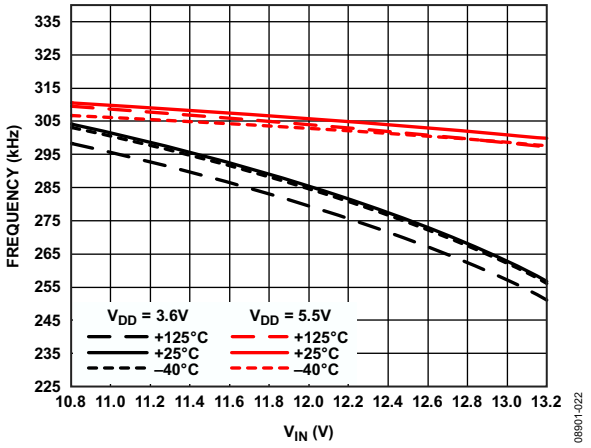

Figure 23. Switching Frequency vs. High Input Voltage, 300 kHz, ±10% of 12 V

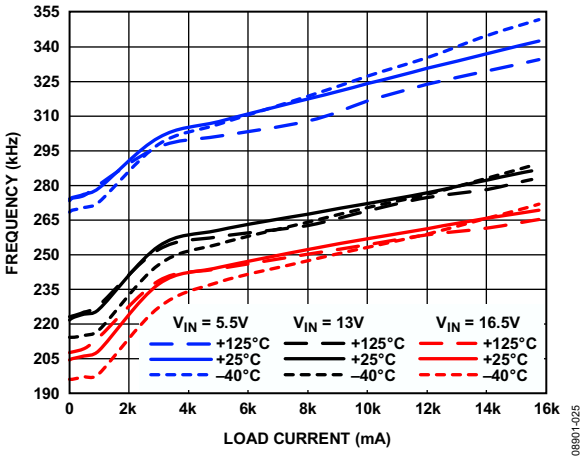

Figure 26. Frequency vs. Load Current, 300 kHz, V_{OUT} = 0.8 V

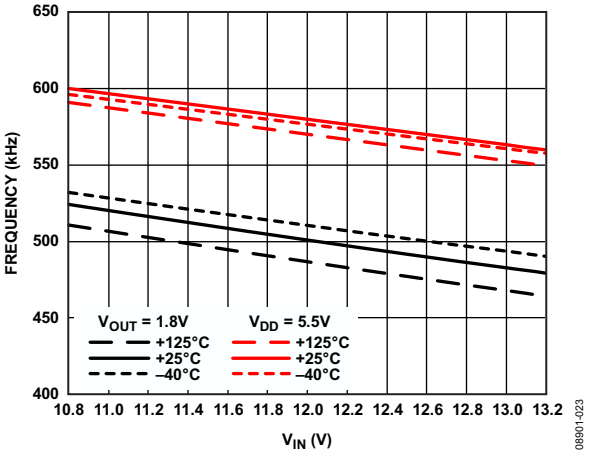

Figure 24. Switching Frequency vs. High Input Voltage, 600 kHz, V_{OUT} = 1.8 V, ±10% of 12 V

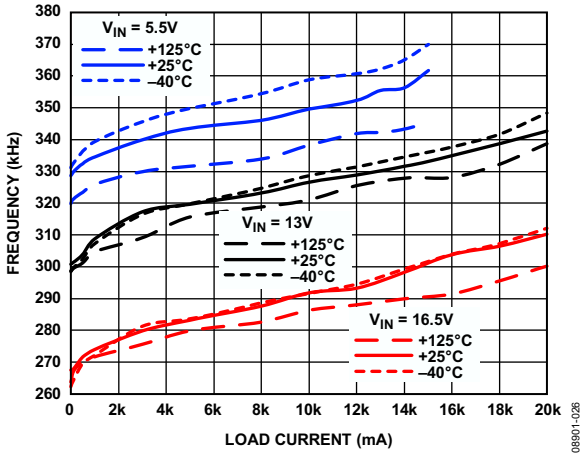

Figure 27. Frequency vs. Load Current, 300 kHz, V_{OUT} = 1.8 V

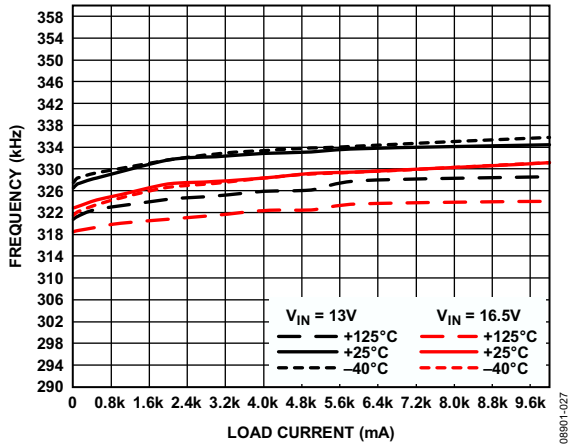

Figure 28. Frequency vs. Load Current, 300 kHz, V_{OUT} = 7 V

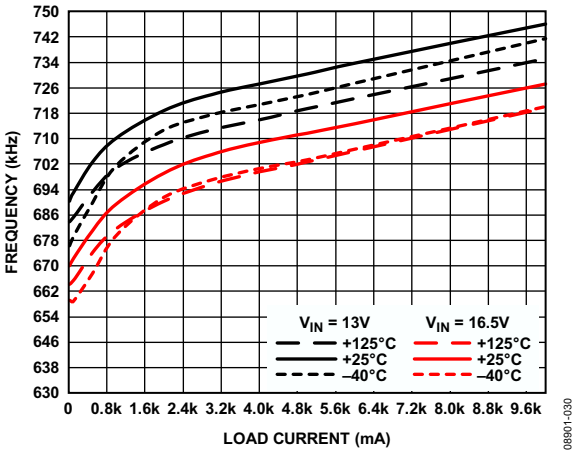

Figure 31. Frequency vs. Load Current, 600 kHz, V_{OUT} =5 V

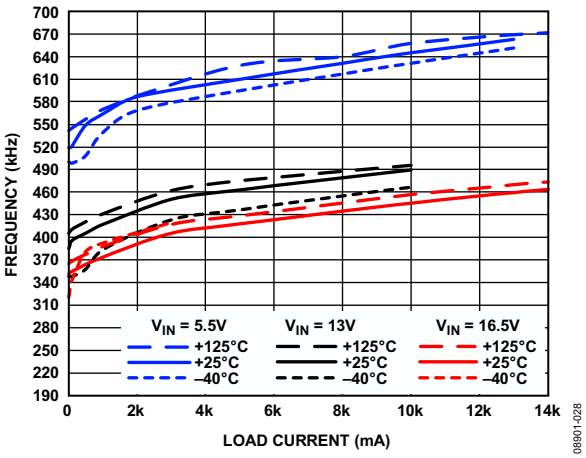

Figure 29. Frequency vs. Load Current, 600 kHz, V_{OUT} = 0.8 V

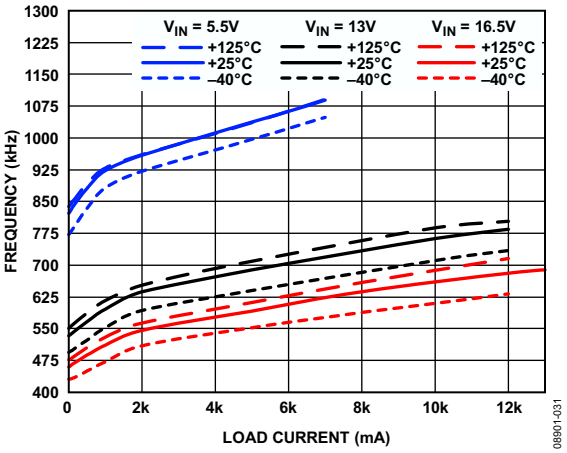

Figure 32. Frequency vs. Load Current, V_{OUT} = 1.0 MHz, 0.8 V

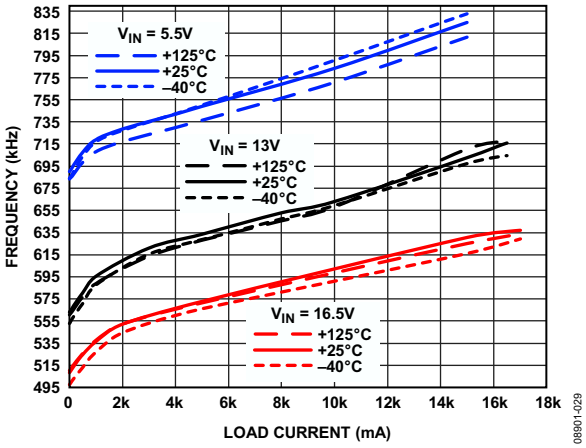

Figure 30. Frequency vs. Load Current, 600 kHz, V_{OUT} = 1.8 V

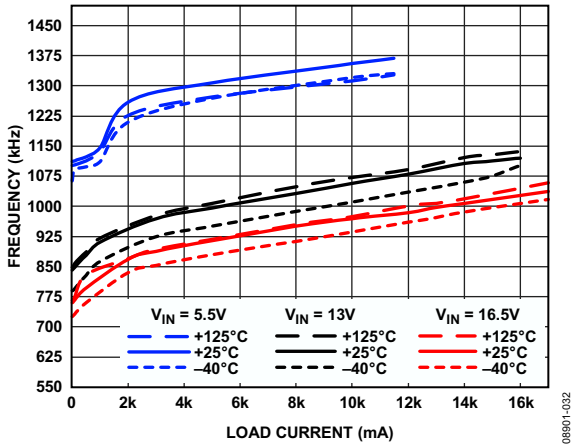

Figure 33. Frequency vs. Load Current, 1.0 MHz, V_{OUT} = 1.8 V

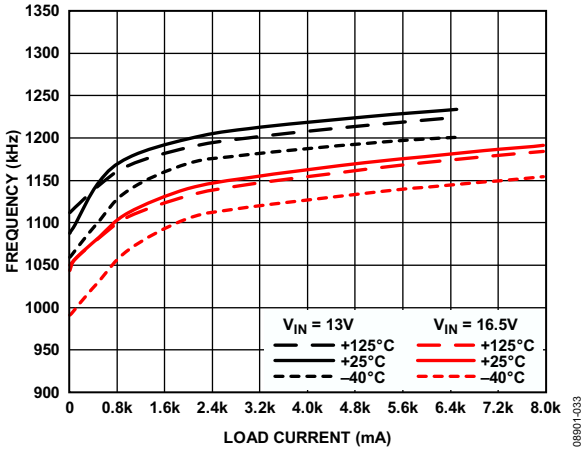

Figure 34. Frequency vs. Load Current, 1.0 MHz, V_{OUT} = 4 V

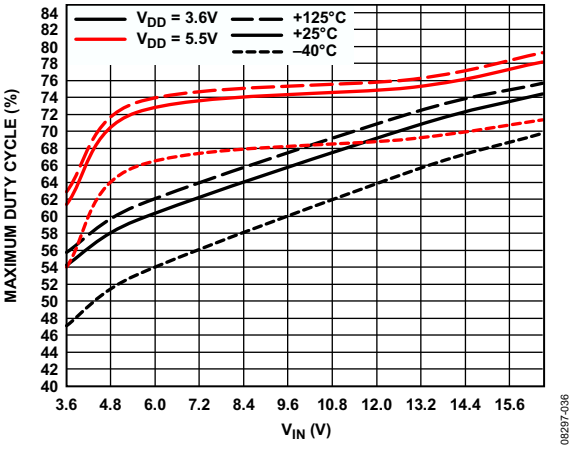

Figure 37. Maximum Duty Cycle vs. High Voltage Input (V_{IN})

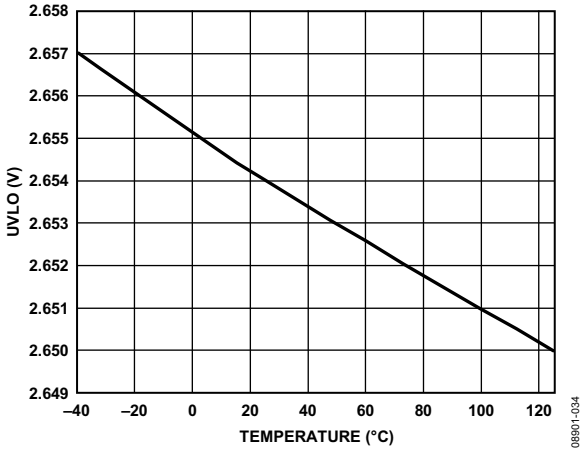

Figure 35. UVLO vs. Temperature

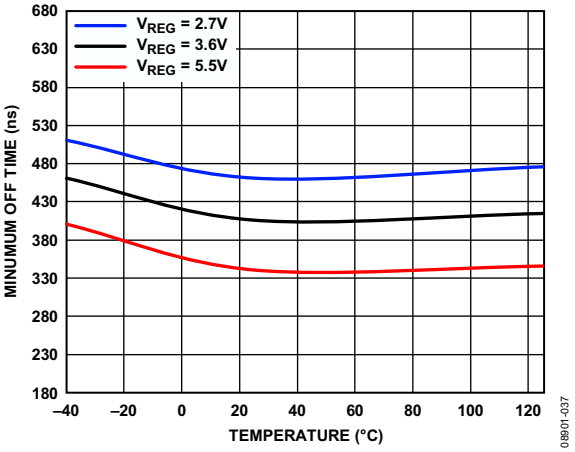

Figure 38. Minimum Off Time vs. Temperature

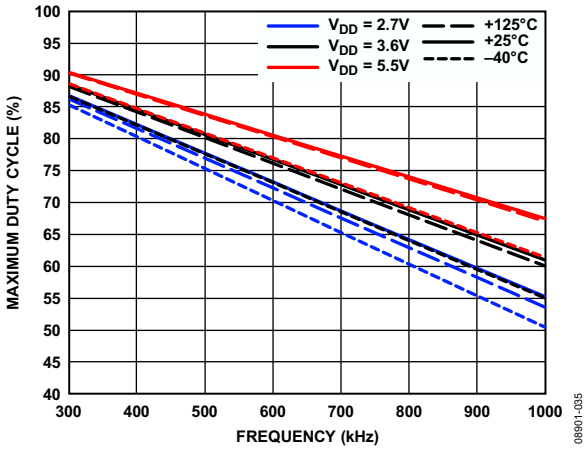

Figure 36. Maximum Duty Cycle vs. Frequency

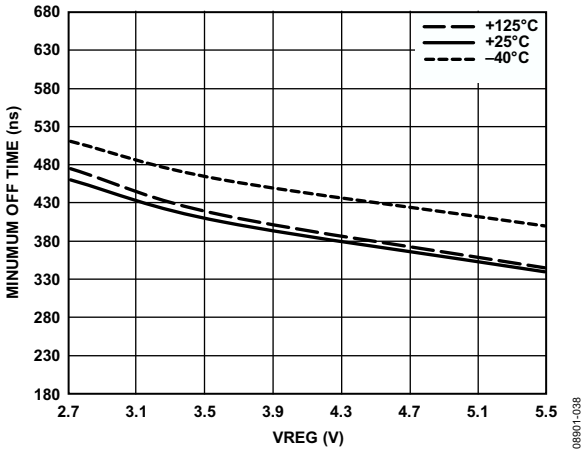

Figure 39. Minimum Off Time vs. V_{DD} (Low Input Voltage)

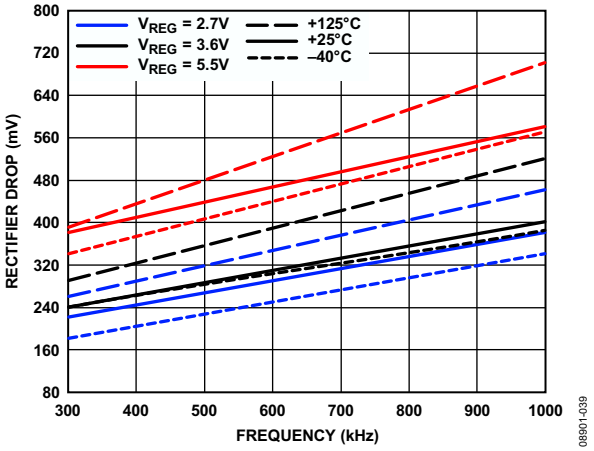

Figure 40. Internal Rectifier Drop vs. Frequency

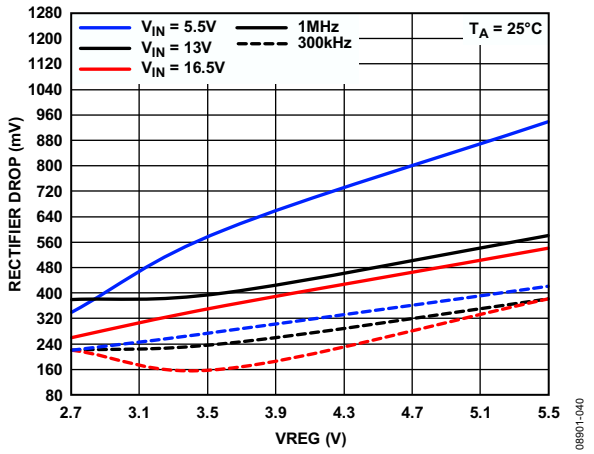

Figure 41. Internal Boost Rectifier Drop vs. V_{DD} (Low Input Voltage) over V_{IN} Variation

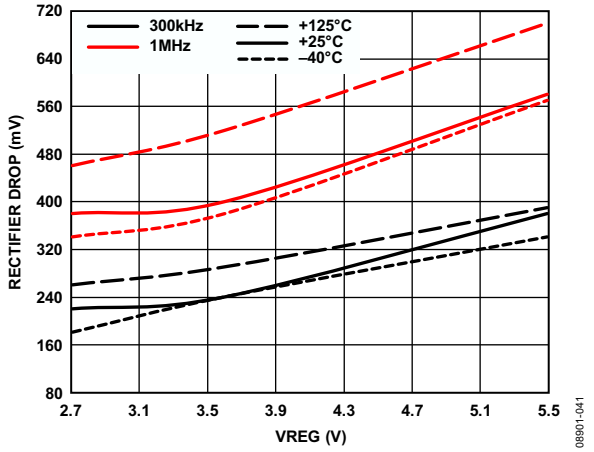

Figure 42. Internal Boost Rectifier Drop vs. V_{DD}

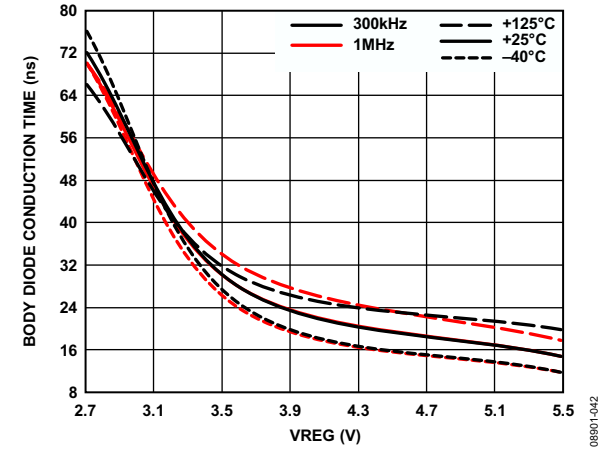

Figure 43. Lower-Side MOSFET Body Conduction Time vs. V_{DD} (Low Input Voltage)

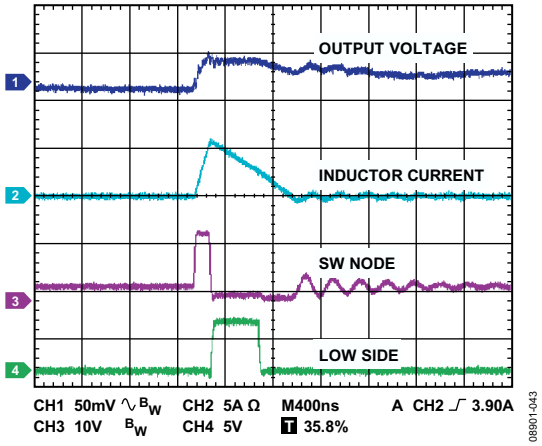

Figure 44. Power Saving Mode (PSM) Operational Waveform, 100 mA

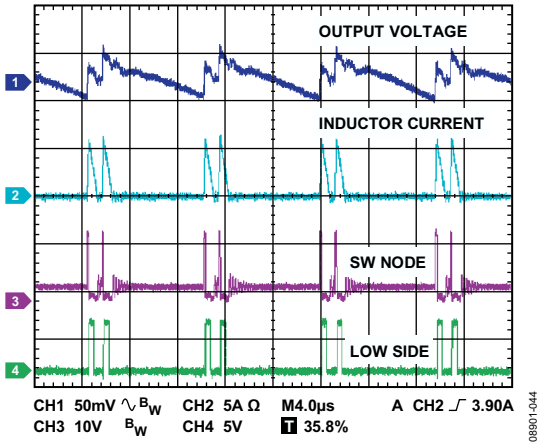

Figure 45. PSM Waveform at Light Load, 500 mA

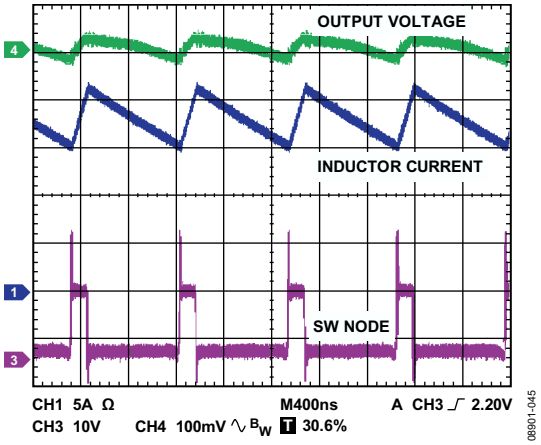

Figure 46. CCM Operation at Heavy Load, 18 A
(See Figure 92 for Applications Circuit)

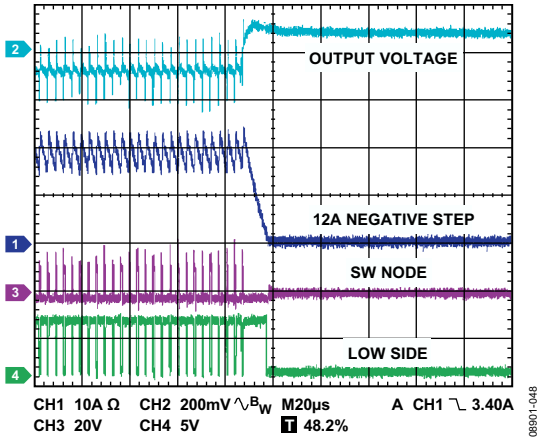

Figure 49. Negative Step During Heavy Load Transient Behavior—PSM Enabled, 20 A (See Figure 92 for Applications Circuit)

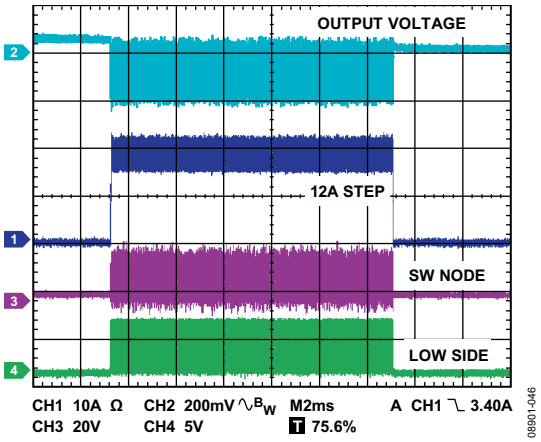

Figure 47. Load Transient Step—PSM Enabled, 20 A
(See Figure 92 for Applications Circuit)

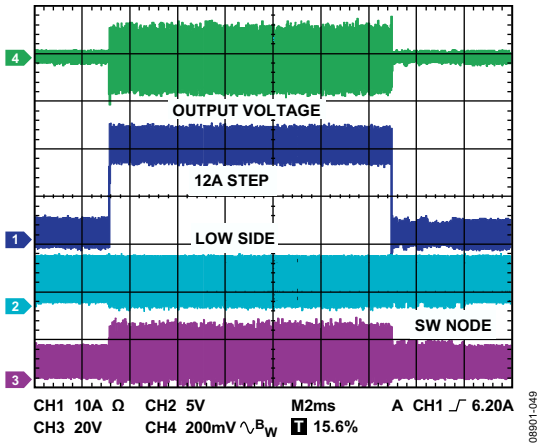

Figure 50. Load Transient Step—Forced PWM at Light Load, 20 A
(See Figure 92 for Applications Circuit)

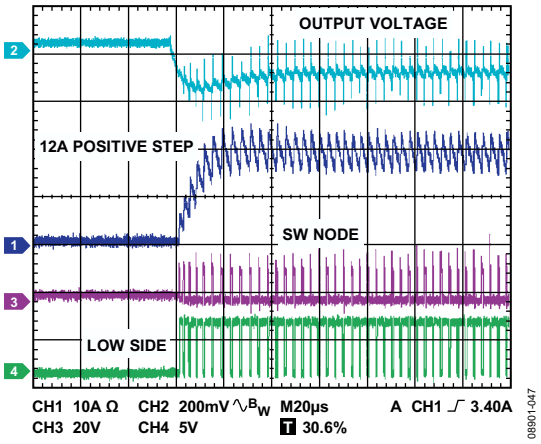

Figure 48. Positive Step During Heavy Load Transient Behavior—PSM Enabled, 20 A, V_{OUT} = 1.8 V (See Figure 92 for Applications Circuit)

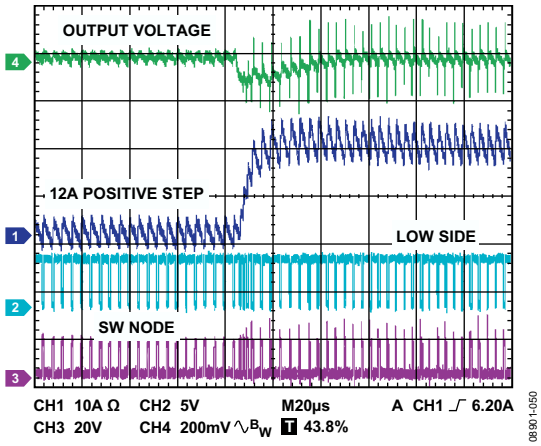

Figure 51. Positive Step During Heavy Load Transient Behavior—Forced PWM at Light Load, 20 A, V_{OUT} = 1.8 V (See Figure 92 for Applications Circuit)

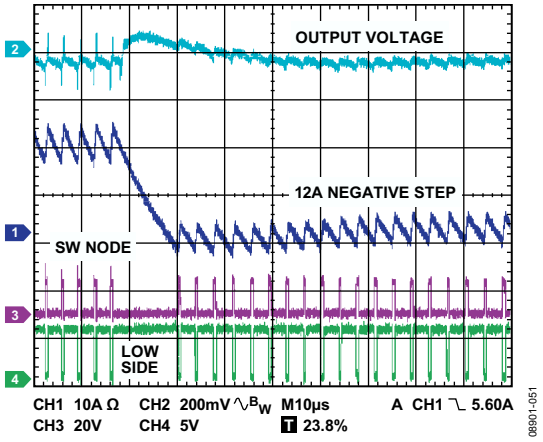

Figure 52. Negative Step During Heavy Load Transient Behavior—Forced PWM at Light Load, 20 A (See Figure 92 for Applications Circuit)

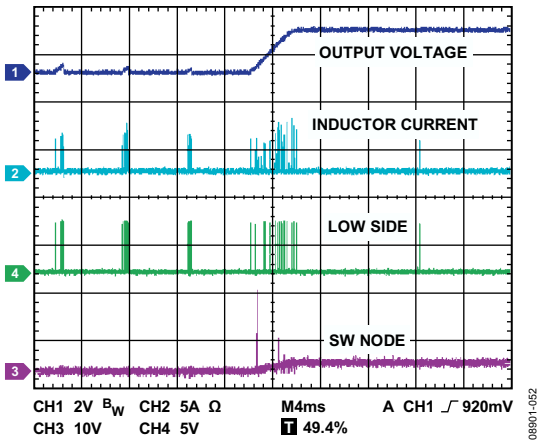

Figure 53. Output Short-Circuit Behavior Leading to Hiccup Mode

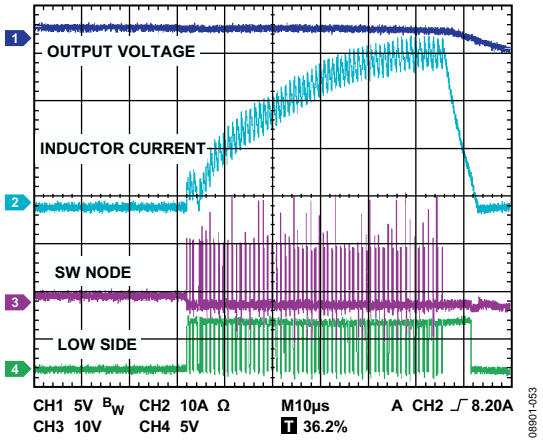

Figure 54. Magnified Waveform During Hiccup Mode

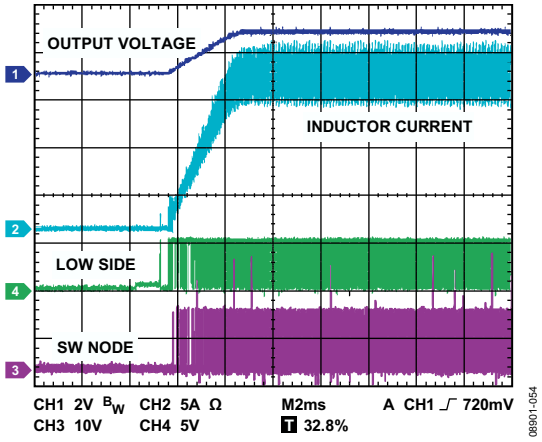

Figure 55. Start-Up Behavior at Heavy Load, 18 A, 300 kHz (See Figure 92 for Applications Circuit)

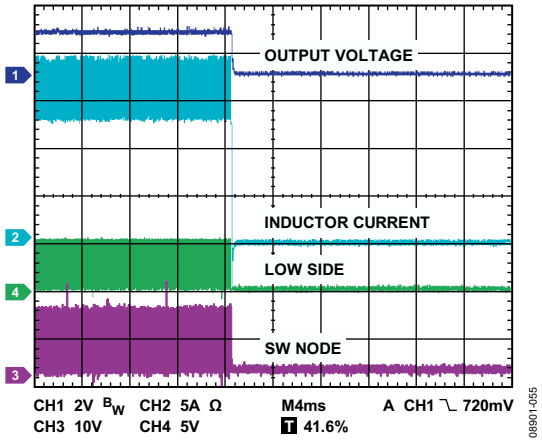

Figure 56. Power-Down Waveform During Heavy Load

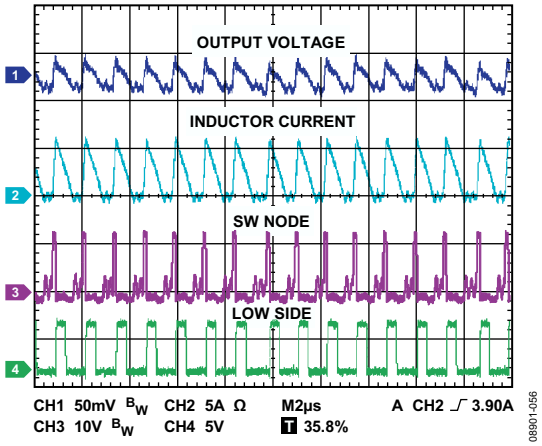

Figure 57. Output Voltage Ripple Waveform During PSM Operation at Light Load, 2 A

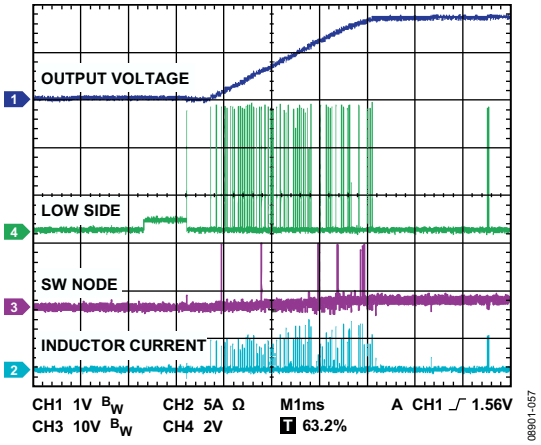

Figure 58. Soft Start and RES Detect Waveform

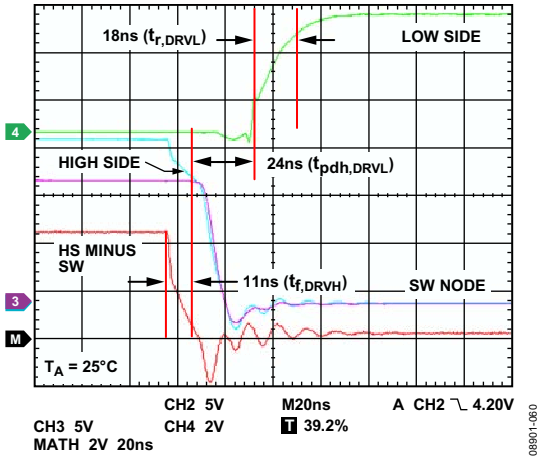

Figure 61. Upper-Side Driver Falling and Lower-Side Rising Edge Waveforms (C_{IN} = 4.3 nF (Upper-Side/Lower-Side MOSFET), Q_{TOTAL} = 27 nC (V_{GS} = 4.4 V (Q1), V_{GS} = 5 V (Q3))

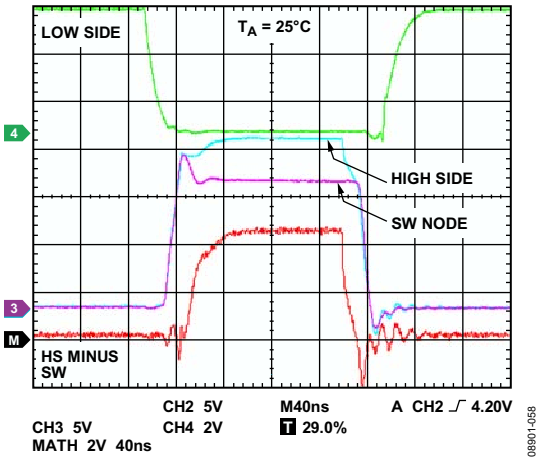

Figure 59. Output Drivers and SW Node Waveforms

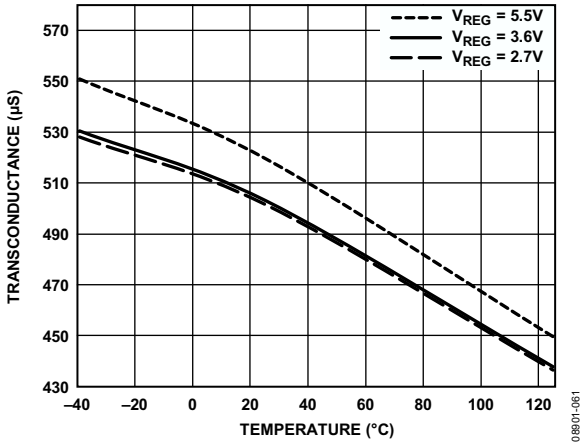

Figure 62. Transconductance (G_M) vs. Temperature

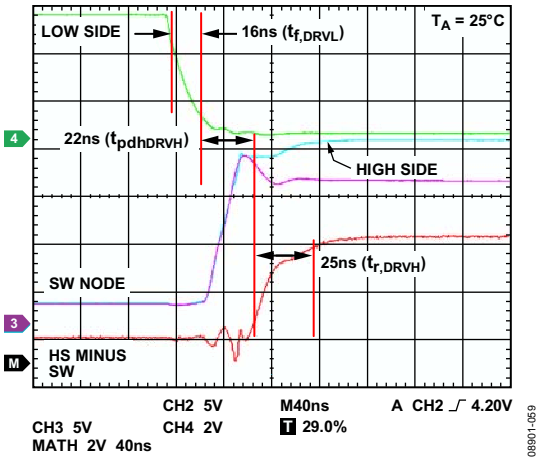

Figure 60. Upper-Side Driver Rising and Lower-Side Falling Edge Waveforms (C_{IN} = 4.3 nF (Upper-Side/Lower-Side MOSFET), Q_{TOTAL} = 27 nC (V_{GS} = 4.4 V (Q1), V_{GS} = 5 V (Q3))

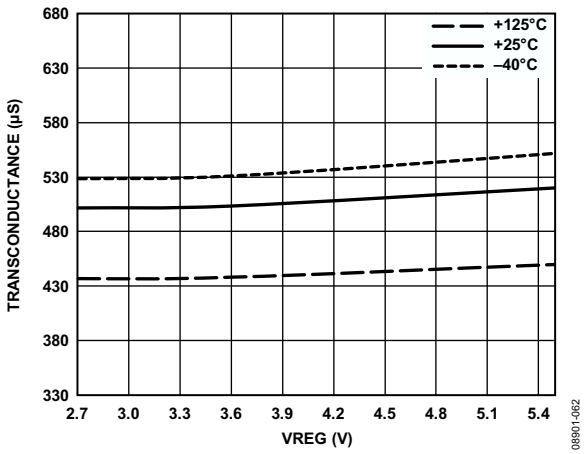

Figure 63. Transconductance (G_M) vs. V_{DD}

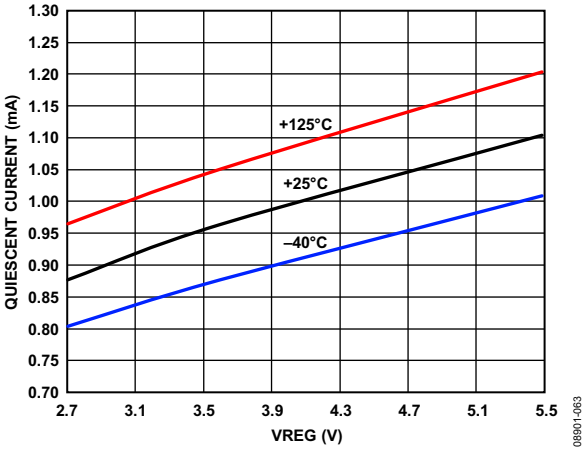

Figure 64. Quiescent Current vs. V_{DD} (V_{IN} = 13 V)

ADP1882/ADP1883 BLOCK DIAGRAM

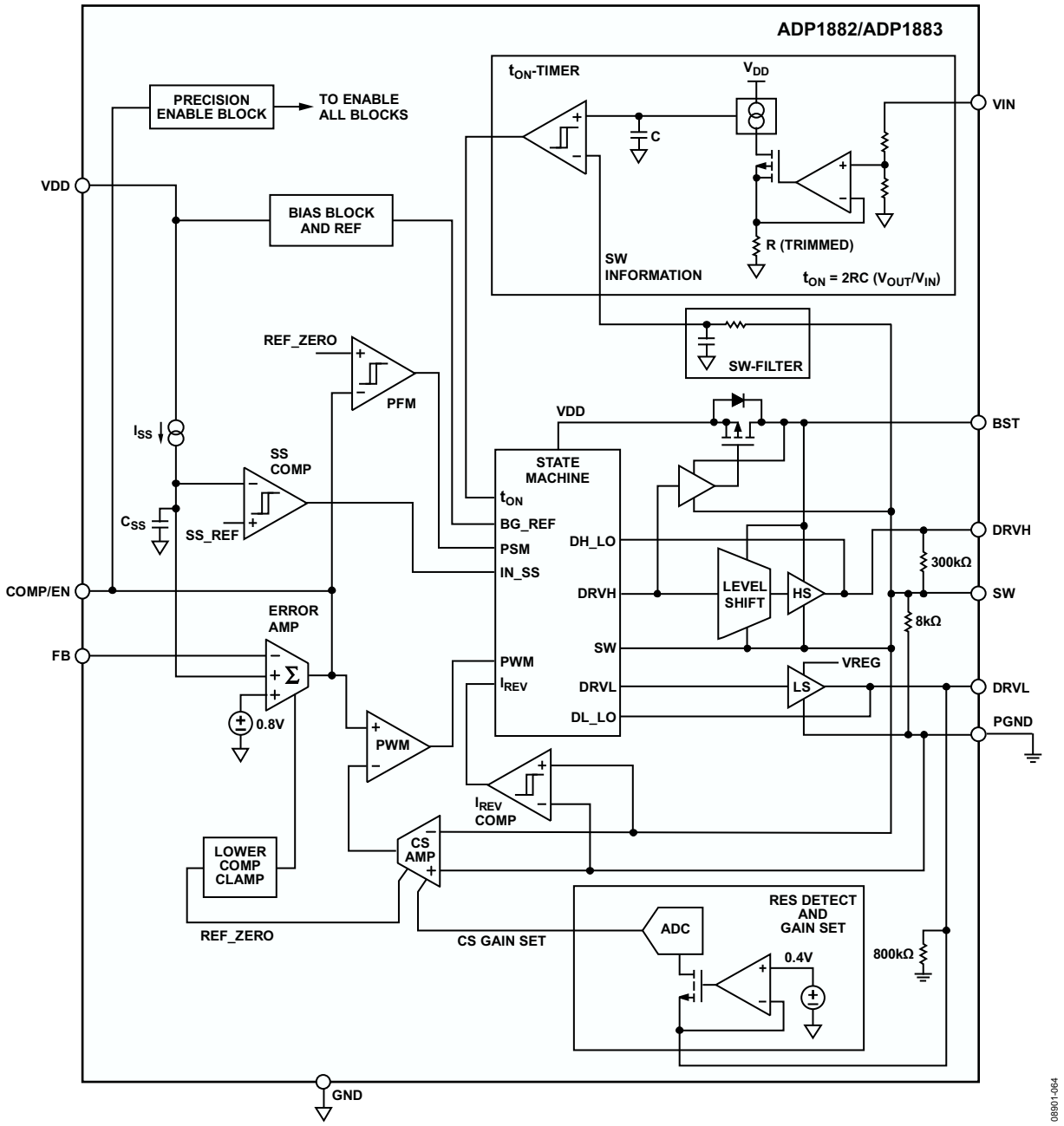

Figure 65. Block Diagram

THEORY OF OPERATION

The ADP1882/ADP1883 are versatile current-mode, synchronous step-down controllers that provide superior transient response, optimal stability, and current limit protection by using a constant on-time, pseudo-fixed frequency with a programmable current-sense gain, current-control scheme. In addition, these devices offer optimum performance at low duty cycles by using valley current-mode control architecture. This allows the ADP1882/ADP1883 to drive all N-channel power stages to regulate output voltages as low as 0.8 V.

STARTUP

The ADP1882/ADP1883 have an input low voltage pin (VDD) for biasing and supplying power for the integrated MOSFET drivers. A bypass capacitor should be located directly across the VDD (Pin 5) and PGND (Pin 7) pins. Included in the power-up sequence is the biasing of the current-sense amplifier, the current-sense gain circuit (see the Programming Resistor (RES) Detect Circuit section), the soft start circuit, and the error amplifier.

The current-sense blocks provide valley current information (see the Programming Resistor (RES) Detect Circuit section) and are a variable of the compensation equation for loop stability (see the Compensation Network section). The valley current information is extracted by forcing 0.4 V across the DRVL output and the PGND pin, which generates a current depending on the resistor across DRVL and PGND in a process performed by the RES detect circuit. The current through the resistor is used to set the current-sense amplifier gain. This process takes approximately 800 µs, after which the drive signal pulses appear at the DRVL and DRVH pins synchronously and the output voltage begins to rise in a controlled manner through the soft start sequence.

The rise time of the output voltage is determined by the soft start and error amplifier blocks (see the Soft Start section). At the beginning of a soft start, the error amplifier charges the external compensation capacitor, causing the COMP/EN pin to rise above the enable threshold of 285 mV, thus enabling the ADP1882/ADP1883.

SOFT START

The ADP1882/ADP1883 have digital soft start circuitry, which involves a counter that initiates an incremental increase in current, by 1 µA, via a current source on every cycle through a fixed internal capacitor. The output tracks the ramping voltage by producing PWM output pulses to the upper-side MOSFET. The purpose is to limit the in-rush current from the high voltage input supply (VIN) to the output (V_{OUT}).

PRECISION ENABLE CIRCUITRY

The ADP1882/ADP1883 employ precision enable circuitry. The enable threshold is 285 mV typical with 35 mV of hysteresis. The devices are enabled when the COMP/EN pin is released, allowing the error amplifier output to rise above the enable threshold (see Figure 66). Grounding this pin disables the ADP1882/ADP1883, reducing the supply current of the devices to approximately 140 µA. For more information, see Figure 67.

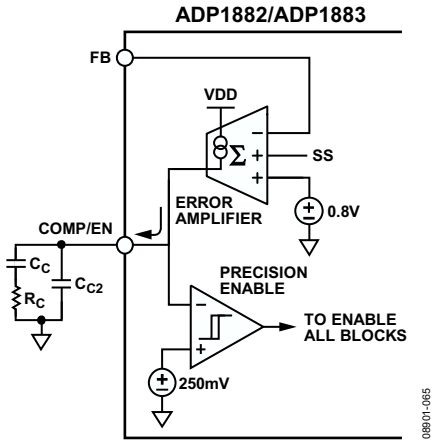

Figure 66. Release COMP/EN Pin to Enable the ADP1882/ADP1883

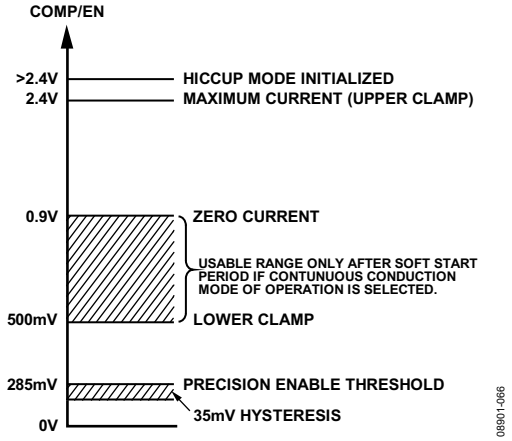

Figure 67. COMP/EN Voltage Range

UNDERVOLTAGE LOCKOUT

The undervoltage lockout (UVLO) feature prevents the part from operating both the upper-side and lower-side MOSFETs at extremely low or undefined input voltage (V_{DD}) ranges. Operation at an undefined bias voltage may result in the incorrect propagation of signals to the high-side power switches. This, in turn, results in invalid output behavior that can cause damage to the output devices, ultimately destroying the device tied at the output. The UVLO level has been set at 2.65 V (nominal).

THERMAL SHUTDOWN

The thermal shutdown is a self-protection feature to prevent the IC from damage due to a very high operating junction temperature. If the junction temperature of the device exceeds 155°C, the part enters the thermal shutdown state. In this state, the device shuts off both the upper-side and lower-side MOSFETs and disables the entire controller immediately, thus reducing the power consumption of the IC. The part resumes operation after the junction temperature of the part cools to less than 140°C.

PROGRAMMING RESISTOR (RES) DETECT CIRCUIT

Upon startup, one of the first blocks to become active is the RES detect circuit. This block powers up before a soft start begins. It forces a 0.4 V reference value at the DRVL output (see Figure 68) and is programmed to identify four possible resistor values: 47 kΩ, 22 kΩ, open, and 100 kΩ.

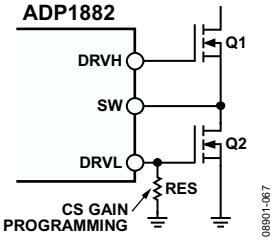

Figure 68. Programming Resistor Location

The RES detect circuit digitizes the value of the resistor at the DRVL pin (Pin 6). An internal ADC outputs a 2-bit digital code that is used to program four separate gain configurations in the current-sense amplifier (see Figure 69). Each configuration corresponds to a current-sense gain (A_{CS}) of 3 V/V, 6 V/V, 12 V/V, and 24 V/V, respectively (see Table 5 and Table 6). This variable is used for the valley current-limit setting, which sets up the appropriate current-sense signal gain for a given application and sets the compensation necessary to achieve loop stability (see the Valley Current-Limit Setting and Compensation Network sections).

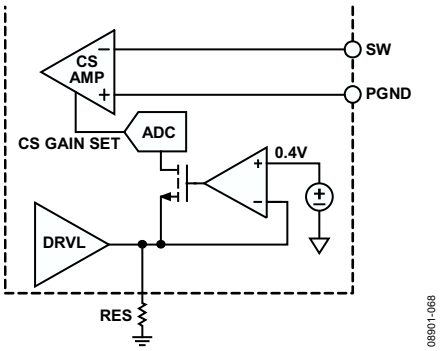

Figure 69. RES Detect Circuit for Current-Sense Gain Programming

Table 5. Current-Sense Gain Programming

Resistor (kΩ)	A_{CS} (V/V)
47	3.25
22	6.5
Open	26
100	13

VALLEY CURRENT-LIMIT SETTING

The architecture of the ADP1882/ADP1883 is based on valley current-mode control. The current limit is determined by three components: the R_{ON} of the lower-side MOSFET, the error amplifier output voltage swing (COMP), and the current-sense gain. The COMP range is internally fixed at 1.5 V. The current-sense gain is programmable via an external resistor at the DRVL pin (see the Programming Resistor (RES) Detect Circuit section). The R_{ON} of the lower-side MOSFET can vary over temperature and usually has a positive T_C (meaning that it increases with temperature); therefore, it is recommended that the current-sense gain resistor be programmed based on the rated R_{ON} of the MOSFET at 125°C.

Because the ADP1882/ADP1883 are based on valley current control, the relationship between I_{CLIM} and I_{LOAD} is as follows:

$$I_{CLIM} = I_{LOAD} \times \left(1 - \frac{K_I}{2}\right)$$

where:
I_{CLIM} is the desired valley current limit.
I_{LOAD} is the current load.
K_I is the ratio between the inductor ripple current and the desired average load current (see Figure 10).

Establishing K_I helps to determine the inductor value (see the Inductor Selection section), but in most cases, K_I = 0.33.

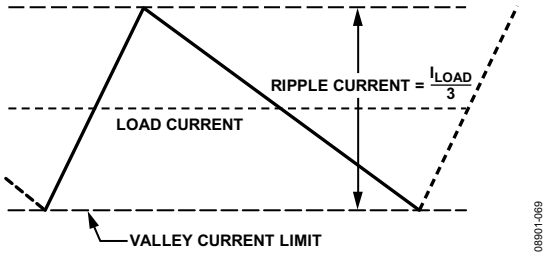

Figure 70. Valley Current Limit to Average Current Relation

When the desired valley current limit (I_{CLIM}) has been determined, the current-sense gain can be calculated by using the following expression:

$$I_{CLIM} = \frac{1.5\ \text{V}}{A_{CS} \times R_{ON}}$$

where:
A_{CS} is the current-sense gain multiplier (see Table 5 and Table 6).
R_{ON} is the channel impedance of the lower-side MOSFET.

Although the ADP1882/ADP1883 have only four discrete current-sense gain settings for a given R_{ON} variable, Table 6 and Figure 71 outline several available options for the valley current setpoint based on various R_{ON} values.

Table 6. Valley Current Limit Program[1]

R_{ON} (mΩ)	Valley Current Level			
	47 kΩ	22 kΩ	Open	100 kΩ
	A_{CS} = 3.4 V/V	A_{CS} = 6.6 V/V	A_{CS} = 26.7 V/V	A_{CS} = 13.4 V/V
1.5				38.5
2				28.8
2.5				23.1
3			38.46	19.2
3.5			32.97	16.5
4.5			25.64	12.8
5			23.08	11.5
5.5			20.98	10.5
10		23.08	11.54	5.77
15	30.769	15.38	7.692	3.85
18	25.641	12.82	6.41	3.21

[1] Refer to Figure 71 for more information and a graphical representation.

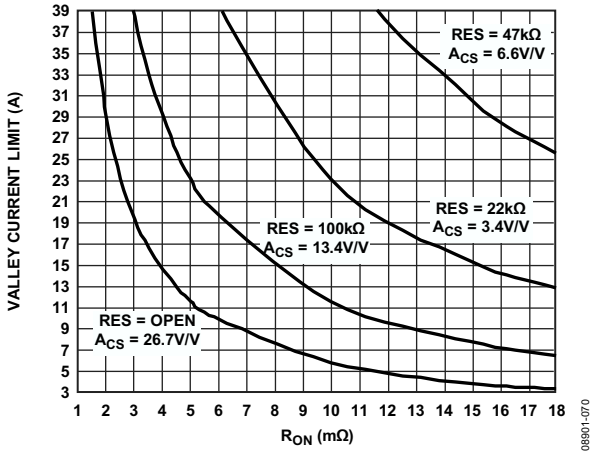

Figure 71. Valley Current-Limit Value vs. R_{ON} of the Lower-Side MOSFET for Each Programming Resistor (RES)

The valley current limit is programmed as outlined in Table 6 and Figure 71. The inductor chosen must be rated to handle the peak current, which is equal to the valley current from Table 6 plus the peak-to-peak inductor ripple current (see the Inductor Selection section). In addition, the peak current value must be used to compute the worst-case power dissipation in the MOSFETs (see Figure 72).

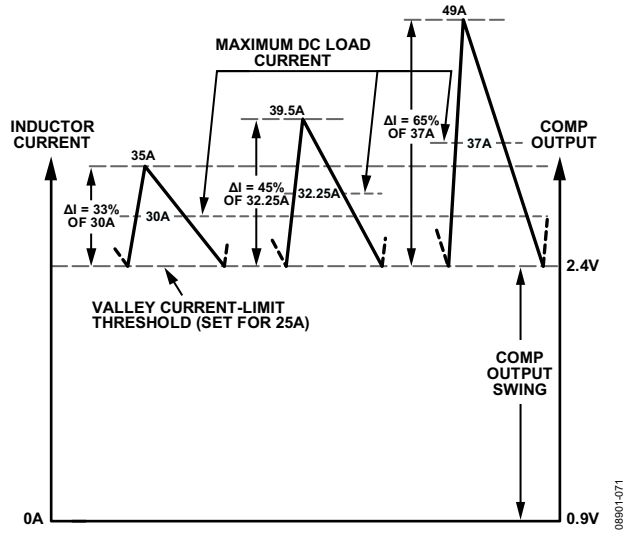

Figure 72. Valley Current-Limit Threshold in Relation to Inductor Ripple Current

HICCUP MODE DURING SHORT CIRCUIT

A current-limit violation occurs when the current across the source and drain of the lower-side MOSFET exceeds the current-limit setpoint. When 32 current-limit violations are detected, the controller enters the idle mode and turns off the MOSFETs for 6 ms, allowing the converter to cool down. Then, the controller reestablishes soft start and begins to cause the output to ramp up again (see Figure 73). While the output ramps up, COMP is monitored to determine if the violation is still present. If it is still present, the idle event occurs again, followed by the full-chip power-down sequence. This cycle continues until the violation no longer exists. If the violation disappears, the converter is allowed to switch normally, maintaining regulation.

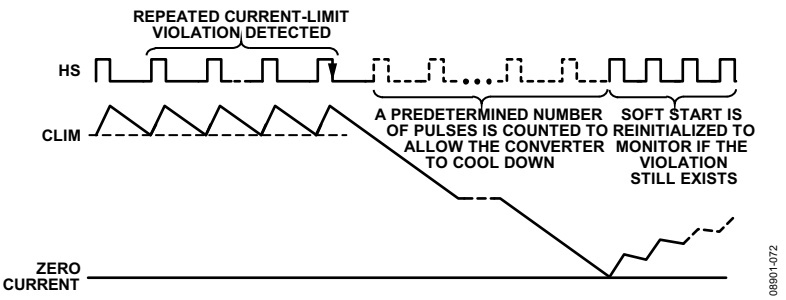

Figure 73. Idle Mode Entry Sequence Due to Current-Limit Violations

SYNCHRONOUS RECTIFIER

The ADP1882/ADP1883 employ an internal lower-side MOSFET driver to drive the external upper-side and lower-side MOSFETs. The synchronous rectifier not only improves overall conduction efficiency but also ensures proper charging to the bootstrap capacitor located at the upper-side driver input. This is beneficial during startup to provide a sufficient drive signal to the external upper-side MOSFET and attain a fast turn on response, which is essential for minimizing switching losses. The integrated upper-side and lower-side MOSFET drivers operate in complementary fashion with built-in anticross conduction circuitry to prevent unwanted shoot-through current that may potentially damage the MOSFETs or reduce efficiency as a result of excessive power loss.

POWER SAVING MODE (PSM) VERSION (ADP1883)

The ADP1883 is the power saving mode version of the ADP1882. The ADP1883 operates in the discontinuous conduction mode (DCM) and pulse skips at light load to midload currents. It outputs pulses, as necessary, to maintain output regulation. Unlike the continuous conduction mode (CCM), DCM operation prevents negative current, thus allowing improved system efficiency at light loads. Current in the reverse direction through this pathway, however, results in power dissipation and, therefore, a decrease in efficiency.

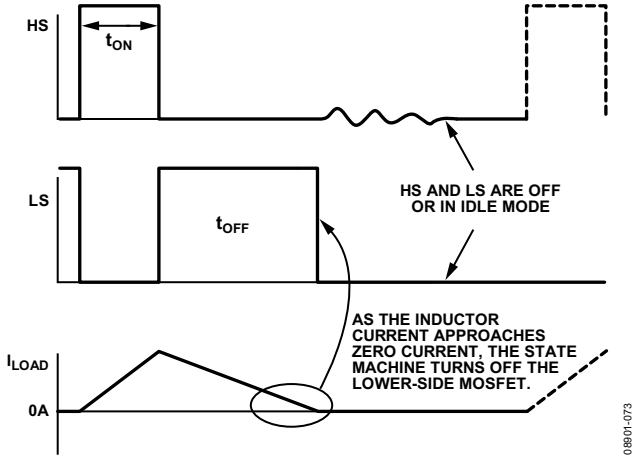

Figure 74. Discontinuous Mode of Operation (DCM)

To minimize the chance of negative inductor current buildup, an on-board, zero-cross comparator turns off all upper-side and lower-side switching activities when the inductor current approaches the zero current line, causing the system to enter idle mode, where the upper-side and lower-side MOSFETs are turned off. To ensure idle mode entry, a 10 mV offset, connected in series at the SW node, is implemented (see Figure 75).

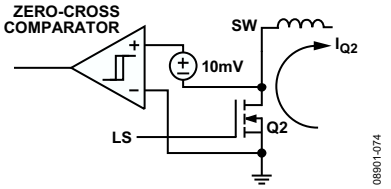

Figure 75. Zero-Cross Comparator with 10 mV of Offset

As soon as the forward current through the lower-side MOSFET decreases to a level where

$$10\ mV = I_{Q2} \times R_{ON(Q2)}$$

the zero-cross comparator (or I_{REV} comparator) emits a signal to turn off the lower-side MOSFET. From this point, the slope of the inductor current ramping down becomes steeper (see Figure 76) as the body diode of the lower-side MOSFET begins to conduct current and continues conducting current until the remaining energy stored in the inductor has been depleted.

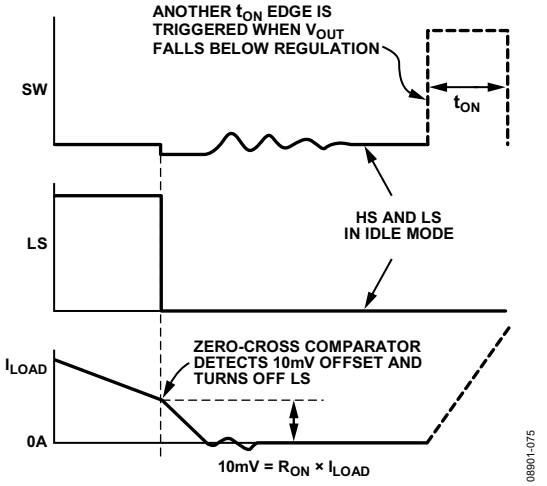

Figure 76. 10 mV Offset to Ensure Prevention of Negative Inductor Current

The system remains in idle mode until the output voltage drops from within regulation. A PWM pulse is then produced, turning on the upper-side MOSFET to maintain system regulation. The ADP1883 does not have an internal clock; therefore, it switches purely as a hysteretic controller as described in this section.

TIMER OPERATION

The ADP1882/ADP1883 employ a constant on-time architecture that provides a variety of benefits, including improved load and line transient responses when compared with a constant (fixed) frequency current-mode control loop of a comparable loop design. The constant on-time timer, or t_{ON} timer, senses the high input voltage (V_{IN}) and the output voltage (V_{OUT}) using SW waveform information to produce an adjustable one-shot PWM pulse that varies the on time of the upper-side MOSFET in response to dynamic changes in input voltage, output voltage, and load current conditions to maintain regulation. It then generates an on-time (t_{ON}) pulse that is inversely proportional to V_{IN}.

$$t_{ON} = K \times \frac{V_{OUT}}{V_{IN}}$$

where K is a constant that is trimmed using an RC timer product for the 300 kHz, 600 kHz, and 1.0 MHz frequency options.

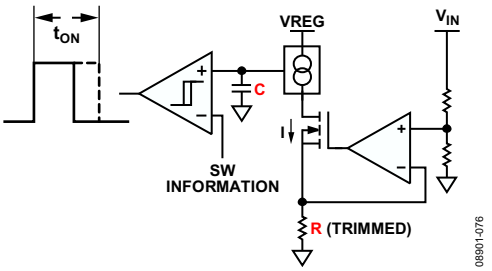

Figure 77. Constant On-Time Timer

The constant on time (t_{ON}) is not strictly constant because it varies with V_{IN} and V_{OUT}. However, this variation occurs in such a way as to keep the switching frequency virtually independent of V_{IN} and V_{OUT}.

The t_{ON} timer uses a feedforward technique, applied to the constant on-time control loop, making it pseudo-fixed frequency to a first order. Second-order effects, such as dc losses in the external power MOSFETs (see the Efficiency Consideration section), cause some variation in frequency vs. load current and line voltage. These effects are shown in Figure 23 to Figure 34. The variations in frequency are much reduced, compared with the variations generated when the feedforward technique is not used.

The feedforward technique establishes the following relationship:

$$f_{SW} = \frac{1}{K}$$

where f_{SW} is the controller switching frequency (300 kHz, 600 kHz, and 1.0 MHz).

The t_{ON} timer senses V_{IN} and V_{OUT} to minimize frequency variation with V_{IN} and V_{OUT} as previously explained. This provides a pseudo fixed frequency that is explained in the Pseudo-Fixed Frequency section. To allow headroom for V_{IN} and V_{OUT} sensing, adhere to the following two equations:

$$V_{DD} \geq V_{IN}/8 + 1.5$$

$$V_{DD} \geq V_{OUT}/4$$

For typical applications where V_{DD} = 5 V, these equations are not relevant; however, for lower V_{DD} inputs, care may be required.

PSEUDO-FIXED FREQUENCY

The ADP1882/ADP1883 employ a constant on-time control scheme. During steady state operation, the switching frequency stays relatively constant, or pseudo-fixed. This is due to the one-shot t_{ON} timer, which produces a high-side PWM pulse with a fixed duration, given that external conditions such as input voltage, output voltage, and load current are also at steady state. During load transients, the frequency momentarily changes for the duration of the transient event so that the output comes back within regulation more quickly than if the frequency were fixed or if it were to remain unchanged. After the transient event is complete, the frequency returns to a pseudo-fixed value to a first-order.

To illustrate this feature more clearly, this section describes one such load transient event—a positive load step—in detail. During load transient events, the high-side driver output pulse width stays relatively consistent from cycle to cycle; however, the off time (DRVL on time) dynamically adjusts according to the instantaneous changes in the external conditions mentioned.

When a positive load step occurs, the error amplifier (out of phase of the output, V_{OUT}) produces new voltage information at its output (COMP). In addition, the current-sense amplifier senses new inductor current information during this positive load transient event. The error amplifier's output voltage reaction is compared to the new inductor current information that sets the start of the next switching cycle. Because current information is produced from valley current sensing, it is sensed at the down ramp of the inductor current, whereas the voltage loop information is sensed through the counter action upswing of the error amplifier's output (COMP).

The result is a convergence of these two signals (see Figure 78), which allows an instantaneous increase in switching frequency during the positive load transient event. In summary, a positive load step causes V_{OUT} to transient down, which causes COMP to transient up and, therefore, shortens the off time. This resultant increase in frequency during a positive load transient helps to quickly bring V_{OUT} back up in value and within the regulation window.

Similarly, a negative load step causes the off time to lengthen in response to V_{OUT} rising. This effectively increases the inductor demagnetizing phase, helping to bring V_{OUT} within regulation. In this case, the switching frequency decreases, or experiences a foldback, to help facilitate output voltage recovery.

Because the ADP1882/ADP1883 can respond rapidly to sudden changes in load demand, the recovery period in which the output voltage settles back to its original steady state operating point is much quicker than it would be for a fixed-frequency equivalent. Therefore, using a pseudo-fixed frequency results in significantly better load transient performance than using a fixed frequency.

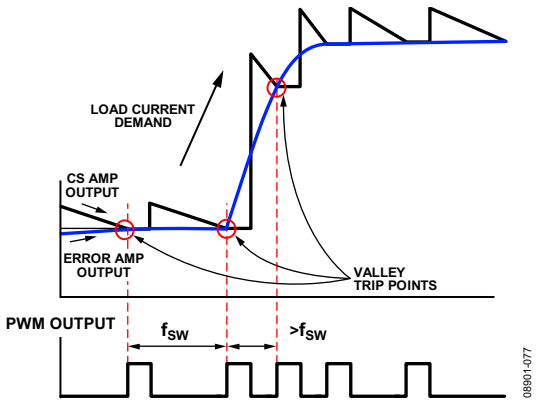

Figure 78. Load Transient Response Operation

APPLICATIONS INFORMATION

FEEDBACK RESISTOR DIVIDER

The required resistor divider network can be determined for a given V_{OUT} value because the internal band gap reference (V_{REF}) is fixed at 0.8 V. Selecting values for R_T and R_B determines the minimum output load current of the converter. Therefore, for a given value of R_B, the R_T value can be determined using the following expression:

$$R_T = R_B \times \frac{(V_{OUT} - 0.8\ \text{V})}{0.8\ \text{V}}$$

INDUCTOR SELECTION

The inductor value is inversely proportional to the inductor ripple current. The peak-to-peak ripple current is given by

$$I_L \quad K_I \quad I_{LOAD} \approx \times = \frac{I_{LOAD}}{3}$$

where K_I is typically 0.33.

The equation for the inductor value is given by

$$L = \frac{(V_{IN} - V_{OUT})}{I_L \times f_{SW}} \times \frac{V_{OUT}}{V_{IN}}$$

where:
V_{IN} is the high voltage input.
V_{OUT} is the desired output voltage.
f_{SW} is the controller switching frequency (300 kHz, 600 kHz, and 1.0 MHz).

When selecting the inductor, choose an inductor saturation rating that is above the peak current level, and then calculate the inductor current ripple (see the Valley Current-Limit Setting section and Figure 79).

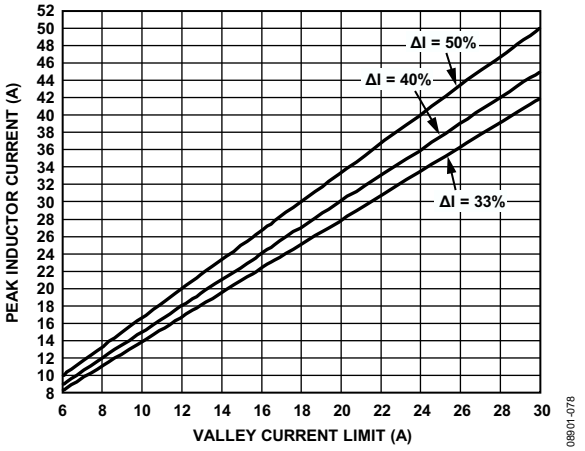

Figure 79. Peak Current vs. Valley Current Threshold for 33%, 40%, and 50% of Inductor Ripple Current

Table 7. Recommended Inductors

L (µH)	DCR (mΩ)	I_{SAT} (A)	Dimensions (mm)	Manufacturer	Model Number
0.12	0.33	55	10.2 × 7	Wurth Electronics	744303012
0.22	0.33	30	10.2 × 7	Wurth Electronics	744303022
0.47	0.8	50	14.2 × 12.8	Wurth Electronics	744355147
0.72	1.65	35	10.5 × 10.2	Wurth Electronics	744325072
0.9	1.6	28	13 × 12.8	Wurth Electronics	744355090
1.2	1.8	25	10.5 × 10.2	Wurth Electronics	744325120
1.0	3.3	20	10.5 × 10.2	Wurth Electronics	7443552100
1.4	3.2	24	14 × 12.8	Wurth Electronics	744318180
2.0	2.6	22	13.2 × 12.8	Wurth Electronics	7443551200
0.8		27.5		Sumida	CEP125U-0R8

OUTPUT RIPPLE VOLTAGE (ΔV_{RR})

The output ripple voltage is the ac component of the dc output voltage during steady state. For a ripple error of 1.0%, the output capacitor value needed to achieve this tolerance can be determined using the following equation. Note that an accuracy of 1.0% is possible only during steady state conditions, not during load transients.

$$\Delta V_{RR} = (0.01) \times V_{OUT}$$

OUTPUT CAPACITOR SELECTION

The primary objective of the output capacitor is to facilitate the reduction of the output voltage ripple; however, the output capacitor also assists in the output voltage recovery during load transient events. For a given load current step, the output voltage ripple generated during this step event is inversely proportional to the value chosen for the output capacitor. The speed at which the output voltage settles during this recovery period depends on where the crossover frequency (loop bandwidth) is set. This crossover frequency is determined by the output capacitor, the equivalent series resistance (ESR) of the capacitor, and the compensation network.

To calculate the small-signal voltage ripple (output ripple voltage) at the steady state operating point, use the following equation:

$$C_{OUT} \quad I_L \times \Delta = \left(\frac{1}{8 \quad F_{SW} \quad [] \ V_{RIPPLE} \quad (\ I_L \times \Delta ESR) \times} \right)$$

where *ESR* is the equivalent series resistance of the output capacitors.

To calculate the output load step, use the following equation:

$$C_{OUT} \quad 2 \times = \frac{\Delta I_{LOAD}}{f_{SW} \quad (\ V_{DROOP} \quad (\ I_{LOAD} \times \Delta ESR))}$$

where ΔV_{DROOP} is the amount that V_{OUT} is allowed to deviate for a given positive load current step (ΔI_{LOAD}).

Ceramic capacitors are known to have low ESR. However, the trade-off of using X5R technology is that up to 80% of its capacitance may be lost due to derating as the voltage applied across the capacitor is increased (see Figure 80). Although X7R series capacitors can also be used, the available selection is limited to only up to 22 µF.

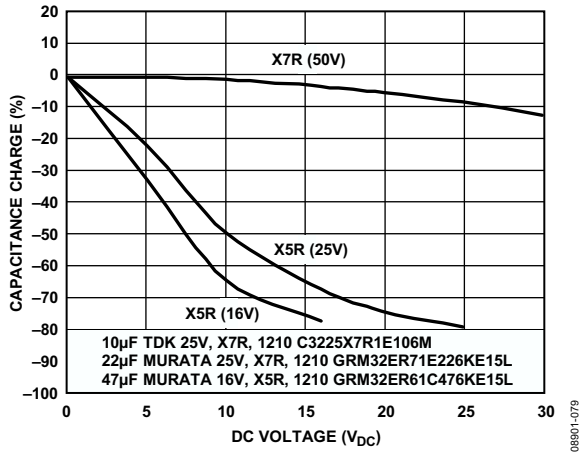

Figure 80. Capacitance vs. DC Voltage Characteristics for Ceramic Capacitors

Electrolytic capacitors satisfy the bulk capacitance requirements for most high current applications. Because the ESR of electrolytic capacitors is much higher than that of ceramic capacitors, when using electrolytic capacitors, several MLCCs should be mounted in parallel to reduce the overall series resistance.

COMPENSATION NETWORK

Due to its current-mode architecture, the ADP1882/ADP1883 require Type II compensation. To determine the component values needed for compensation (resistance and capacitance values), it is necessary to examine the overall loop gain (H) of the converter at the unity gain frequency ($f_{SW}/10$) when H = 1 V/V, as follows:

$$H = 1\ \text{V/V} = G_M \times A_{CS} \times \frac{V_{OUT}}{V_{REF}} \times Z_{COMP} \times Z_{FILT}$$

Examining each variable at high frequency enables the unity-gain transfer function to be simplified to provide expressions for the R_{COMP} and C_{COMP} component values.

Output Filter Impedance (Z_{FILT})

Examining the transfer function of the filter at high frequencies simplifies to

$$Z_{FILT} = \frac{1}{sC_{OUT}}$$

at the crossover frequency ($s = 2\pi f_{CROSS}$).

Error Amplifier Output Impedance (Z_{COMP})

Assuming C_{C2} is significantly smaller than C_{COMP}, C_{C2} can be omitted from the output impedance equation of the error amplifier. The transfer function simplifies to

$$Z_{COMP} = \frac{R_{COMP}(f_{CROSS} + f_{ZERO})}{f_{CROSS}}$$

and

$$f_{CROSS} \quad \frac{1}{12} \times f_{SW}$$

where f_{ZERO}, the zero frequency, is set to be 1/4 of the crossover frequency for the ADP1882.

Error Amplifier Gain (G_M)

The error amplifier gain (transconductance) is

$$G_M = 500\ \mu\text{A/V}$$

Current-Sense Loop Gain (G_{CS})

The current-sense loop gain is

$$G_{CS} = \frac{1}{A_{CS} \times R_{ON}}\ \text{(A/V)}$$

where:
A_{CS} (V/V) is programmable for 3 V/V, 6 V/V, 12 V/V, and 24 V/V (see the Programming Resistor (RES) Detect Circuit and Valley Current-Limit Setting sections).
R_{ON} is the channel impedance of the lower-side MOSFET.

Crossover Frequency

The crossover frequency is the frequency at which the overall loop (system) gain is 0 dB (H = 1 V/V). For current-mode converters such as the ADP1882, it is recommended that the user set the crossover frequency between 1/10 and 1/15 of the switching frequency.

$$f_{CROSS} = \frac{1}{12} f_{SW}$$

The relationship between C_{COMP} and f_{ZERO} (zero frequency) is as follows:

$$f_{ZERO} = \frac{1}{2 \quad R_{COMP} \times C_{COMP}})$$

The zero frequency is set to 1/4 of the crossover frequency.

Combining all of the above parameters results in

$$R_{COMP} = \frac{f_{CROSS}}{f_{CROSS} + f_{ZERO}} \times \frac{2\pi f_{CROSS} C_{OUT}}{G_M A_{CS}} \times \frac{V_{OUT}}{V_{REF}}$$

$$C_{COMP} = \frac{1}{2 \quad R_{COMP} \times f_{ZERO}}$$

EFFICIENCY CONSIDERATIONS

One of the important criteria to consider in constructing a dc-to-dc converter is efficiency. By definition, efficiency is the ratio of the output power to the input power. For high power applications at load currents up to 20 A, the following are important MOSFET parameters that aid in the selection process:

- $V_{GS\,(TH)}$, the MOSFET support voltage applied between the gate and the source
- $R_{DS\,(ON)}$, the MOSFET on resistance during channel conduction
- Q_G, the total gate charge
- C_{N1}, the input capacitance of the upper-side switch
- C_{N2}, the input capacitance of the lower-side switch

The following are the losses experienced through the external component during normal switching operation:

- Channel conduction loss (both MOSFETs)
- MOSFET driver loss
- MOSFET switching loss
- Body diode conduction loss (lower-side MOSFET)
- Inductor loss (copper and core loss)

Channel Conduction Loss

During normal operation, the bulk of the loss in efficiency is due to the power dissipated through MOSFET channel conduction. Power loss through the upper-side MOSFET is directly proportional to the duty cycle (D) for each switching period, and the power loss through the lower-side MOSFET is directly proportional to 1 − D for each switching period. The selection of MOSFETs is governed by the amount of maximum dc load current that the converter is expected to deliver. In particular, the selection of the lower-side MOSFET is dictated by the maximum load current because a typical high current application employs duty cycles of less than 50%. Therefore, the lower-side MOSFET is in the on state for most of the switching period.

$$P_{N1,N2(CL)} \quad \left[D \quad R_{N1(ON)} \quad () \quad D \quad R_{N2(ON)}\right] \times I^2_{LOAD} \times =$$

MOSFET Driver Loss

Other dissipative elements are the MOSFET drivers. The contributing factors are the dc current flowing through the driver during operation and the Q_{GATE} parameter of the external MOSFETs.

$$P_{DR(LOSS)} \quad \left[V_{DR} \times \left(f_{SW} C_{upperFET} V_{DR} + I_{BIAS}\right)\right]$$
$$\left[V_{DD} \times \left(f_{SW} C_{lowerFET} V_{DD} + I_{BIAS}\right)\right.$$

where:
V_{DR} is the driver bias voltage (that is, the low input voltage (V_{DD}) minus the rectifier drop (see Figure 81)).
$C_{upperFET}$ is the input gate capacitance of the upper-side MOSFET.
$C_{lowerFET}$ is the input gate capacitance of the lower-side MOSFET.
I_{BIAS} is the dc current flowing into the upper and lower-side drivers.
V_{DD} is the bias voltage.

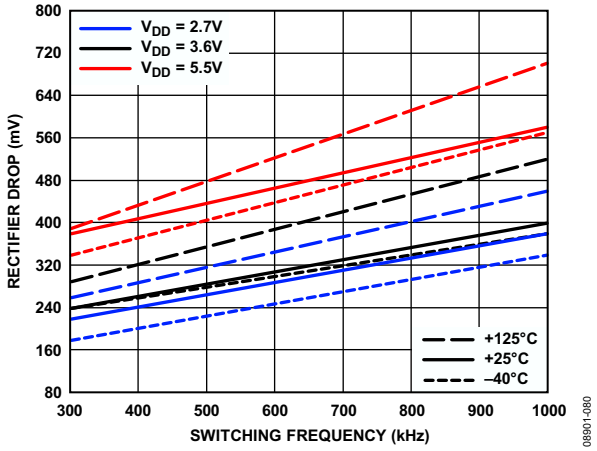

Figure 81. Internal Rectifier Voltage Drop vs. Switching Frequency

Switching Loss

The SW node transitions as a result of the switching activities of the upper-side and lower-side MOSFETs. This causes removal and replenishing of charge to and from the gate oxide layer of the MOSFET, as well as to and from the parasitic capacitance that is associated with the gate oxide edge overlap and the drain and source terminals. The current that enters and exits these charge paths presents additional loss during these transition times. This loss can be approximately quantified by using the following equation, which represents the time in which charge enters and exits these capacitive regions:

$$t_{SW\text{-}TRANS} = R_{GATE} \times C_{TOTAL}$$

where:
R_{GATE} is the gate input resistance of the MOSFET.
C_{TOTAL} is the C_{GD} + C_{GS} of the external MOSFET used.

The ratio of this time constant to the period of one switching cycle is the multiplying factor to be used in the following expression:

$$P_{SW(LOSS)} = \frac{t_{SW\text{-}TRANS}}{t_{SW}} \quad I_{LOAD} \quad V_{IN} \times 2 \times$$

or

$$P_{SW(LOSS)} = f_{SW} \times R_{GATE} \times C_{TOTAL} \times I_{LOAD} \times V_{IN} \times 2$$

Diode Conduction Loss

The ADP1882/ADP1883 employ anticross conduction circuitry that prevents the upper-side and lower-side MOSFETs from conducting current simultaneously. This overlap control is beneficial, avoiding large current flow that may lead to irreparable damage to the external components of the power stage. However, this blanking period comes with the trade-off of a diode conduction loss occurring immediately after the MOSFETs change states and continuing well into idle mode. The amount of loss through the body diode of the lower-side MOSFET during the antioverlap state is given by the following expression:

$$P_{BODY(LOSS)} = \frac{t_{BODY(LOSS)}}{t_{SW}} \quad I_{LOAD} \quad V_F \times 2 \times$$

where:

$t_{BODY(LOSS)}$ is the body conduction time (refer to Figure 82 for dead time periods).

t_{SW} is the period per switching cycle.

V_F is the forward drop of the body diode during conduction (refer to the selected external MOSFET data sheet for more information about the V_F parameter).

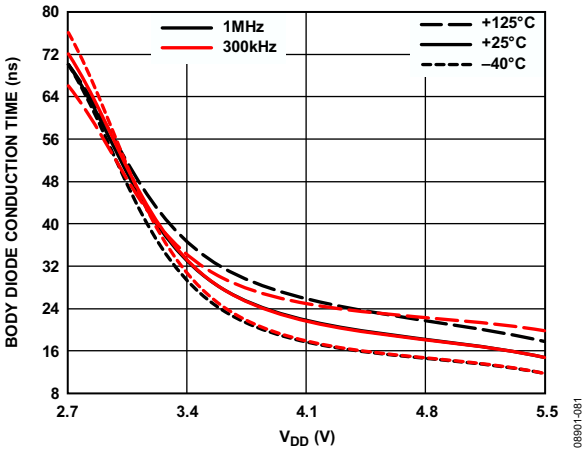

Figure 82. Body Diode Conduction Time vs. Low Voltage Input (V_{DD})

Inductor Loss

During normal conduction mode, further power loss is caused by the conduction of current through the inductor windings, which have dc resistance (DCR). Typically, larger sized inductors have smaller DCR values.

The inductor core loss is a result of the eddy currents generated within the core material. These eddy currents are induced by the changing flux, which is produced by the current flowing through the windings. The amount of inductor core loss depends on the core material, the flux swing, the frequency, and the core volume. Ferrite inductors have the lowest core losses, whereas powdered iron inductors have higher core losses. It is recommended to use shielded ferrite core material type inductors with the ADP1882/ADP1883 for a high current, dc-to-dc switching application to achieve minimal loss and negligible electromagnetic interference (EMI).

$$P_{DCR(LOSS)} = DCR \times I^2_{LOAD} + Core\ Loss$$

INPUT CAPACITOR SELECTION

The goal in selecting an input capacitor is to reduce or minimize input voltage ripple and to reduce the high frequency source impedance, which is essential for achieving predictable loop stability and transient performance.

The problem with using bulk capacitors, other than their physical geometries, is their large equivalent series resistance (ESR) and large equivalent series inductance (ESL). Aluminum electrolytic capacitors have such high ESR that they cause undesired input voltage ripple magnitudes and are generally not effective at high switching frequencies.

If bulk capacitors are to be used, it is recommended that multilayered ceramic capacitors (MLCC) be used in parallel, due to their low ESR values. This dramatically reduces the input voltage ripple amplitude as long as the MLCCs are mounted directly across the drain of the upper-side MOSFET and the source terminal of the lower-side MOSFET (see the Layout Considerations section). Improper placement and mounting of these MLCCs may cancel their effectiveness due to stray inductance and an increase in trace impedance.

$$I_{CIN,RMS} = I_{LOAD,MAX} \times \frac{\sqrt{V_{OUT} \quad (V_{IN} - V_{OUT}}}{V_{OUT}}$$

The maximum input voltage ripple and maximum input capacitor rms current occur at the end of the duration of 1 − D while the upper-side MOSFET is in the off state. The input capacitor rms current reaches its maximum at Time D. When calculating the maximum input voltage ripple, account for the ESR of the input capacitor as follows:

$$V_{MAX,RIPPLE} = V_{RIPP} + (I_{LOAD,MAX} \times ESR)$$

where:

V_{RIPP} is usually 1% of the minimum voltage input.

$I_{LOAD,MAX}$ is the maximum load current.

ESR is the equivalent series resistance rating of the input capacitor used.

Inserting $V_{MAX,RIPPLE}$ into the charge balance equation to calculate the minimum input capacitor requirement gives

$$C_{IN,min} = \frac{I_{LOAD,MAX}}{V_{MAX,RIPPLE}} \times \frac{D(1-D)}{f_{SW}}$$

or

$$C_{IN,min} = \frac{I_{LOAD,MAX}}{4 f_{SW} V_{MAX,RIPPLE}}$$

where D = 50%.

THERMAL CONSIDERATIONS

The ADP1882/ADP1883 are used for dc-to-dc, step down, high current applications that have an on-board controller and on-board MOSFET drivers. Because applications may require up to 20 A of load current delivery and be subjected to high ambient temperature surroundings, the selection of external upper-side and lower-side MOSFETs must be associated with careful thermal consideration to not exceed the maximum allowable junction temperature of 125°C. To avoid permanent or irreparable damage if the junction temperature reaches or exceeds 155°C, the part enters thermal shutdown, turning off both external MOSFETs, and does not reenable until the junction temperature cools to 140°C (see the Thermal Shutdown section).

The maximum junction temperature allowed for the ADP1882/ADP1883 ICs is 125°C. This means that the sum of the ambient temperature (T_A) and the rise in package temperature (T_R), which is caused by the thermal impedance of the package and the internal power dissipation, should not exceed 125°C, as dictated by the following expression:

$$T_J = T_R \times T_A$$

where:
T_A is the ambient temperature.
T_J is the maximum junction temperature.
T_R is the rise in package temperature due to the power dissipated from within.

The rise in package temperature is directly proportional to its thermal impedance characteristics. The following equation represents this proportionality relationship:

$$T_R = \theta_{JA} \times P_{DR(LOSS)}$$

where:
θ_{JA} is the thermal resistance of the package from the junction to the outside surface of the die, where it meets the surrounding air.
$P_{DR(LOSS)}$ is the overall power dissipated by the IC.

The bulk of the power dissipated is due to the gate capacitance of the external MOSFETs. The power loss equation of the MOSFET drivers (see the MOSFET Driver Loss section in the Efficiency Consideration section) is

$$P_{DR(LOSS)} = [V_{DR} \times (f_{SW}C_{upperFET}V_{DR} + I_{BIAS})] + [V_{DD} \times (f_{SW}C_{lowerFET}V_{DD} + I_{BIAS})]$$

where:
$C_{upperFET}$ is the input gate capacitance of the upper-side MOSFET.
$C_{lowerFET}$ is the input gate capacitance of the lower-side MOSFET.
I_{BIAS} is the dc current (2 mA) flowing into the upper-side and lower-side drivers.
V_{DR} is the driver bias voltage (that is, the low input voltage (V_{DD}) minus the rectifier drop (see Figure 81)).
V_{DD} is the bias voltage

For example, if the external MOSFET characteristics are θ_{JA} (10-lead MSOP) = 171.2°C/W, f_{SW} = 300 kHz, I_{BIAS} = 2 mA, $C_{upperFET}$ = 3.3 nF, $C_{lowerFET}$ = 3.3 nF, V_{DR} = 5.12 V, and V_{DD} = 5.5 V, then the power loss is

$$P_{DR(LOSS)} = [V_{DR} \times (f_{SW}C_{upperFET}V_{DR} + I_{BIAS})] + [V_{DD} \times (f_{SW}C_{lowerFET}V_{DD} + I_{BIAS})]$$
$$= [5.12 \times (300 \times 10^3 \times 3.3 \times 10^{-9} \times 5.12 + 0.002)] + [5.5 \times (300 \times 10^3 \times 3.3 \times 10^{-9} \times 5.5 + 0.002)]$$
$$= 77.13 \text{ mW}$$

The rise in package temperature is

$$T_R = \theta_{JA} \times P_{DR(LOSS)}$$
$$= 171.2°C \times 77.13 \text{ mW}$$
$$= 13.2°C$$

Assuming a maximum ambient temperature environment of 85°C, the junction temperature is

$$T_J = T_R \times T_A = 13.2°C + 85°C = 98.2°C$$

which is below the maximum junction temperature of 125°C.

DESIGN EXAMPLE

The ADP1882/ADP1883 are easy to use, requiring only a few design criteria. For example, the example outlined in this section uses only four design criteria: V_{OUT} = 1.8 V, I_{LOAD} = 15 A (pulsing), V_{IN} = 12 V (typical), and f_{SW} = 300 kHz.

Input Capacitor

The maximum input voltage ripple is usually 1% of the minimum input voltage (11.8 V × 0.01 = 120 mV).

$$V_{RIPP} = 120 \text{ mV}$$

$$V_{MAX,RIPPLE} = V_{RIPP} - (I_{LOAD,MAX} \times ESR)$$
$$= 120 \text{ mV} - (15 \text{ A} \times 0.001) = 45 \text{ mV}$$

$$C_{IN,min} = \frac{I_{LOAD,MAX}}{4 f_{SW} V_{MAX,RIPPLE}} = \frac{15 \text{ A}}{4 \quad 300 \quad 10^3 \times 105 \text{ mV}}$$
$$= 120 \text{ µF}$$

Choose five 22 µF ceramic capacitors. The overall ESR of five 22 µF ceramic capacitors is less than 1 mΩ.

$$I_{RMS} = I_{LOAD}/2 = 7.5 \text{ A}$$

$$P_{CIN} = (I_{RMS})^2 \times ESR = (7.5\text{A})^2 \times 1 \text{ m}\Omega = 56.25 \text{ mW}$$

Inductor

Determine the inductor ripple current amplitude as follows:

$$I_L \approx \frac{\Delta I_{LOAD}}{3} = 5 \text{ A}$$

then calculate for the inductor value

$$L = \frac{(V_{IN,MAX} - V_{OUT})}{I_L \times f_{SW}} \times \frac{V_{OUT}}{V_{IN,MAX}}$$

$$= \frac{(13.2 \text{ V} - 1.8 \text{ V})}{5 \text{ V} \quad 300 \times 10^3} \times \frac{1.8 \text{ V}}{13.2 \text{ V}}$$

$$= 1.03 \text{ µH}$$

The inductor peak current is approximately

$$15 \text{ A} + (5 \text{ A} \times 0.5) = 17.5 \text{ A}$$

Therefore, an appropriate inductor selection is 1.0 µH with DCR = 3.3 mΩ (7443552100) from Table 8, with peak current handling of 20 A.

$$P_{DCR(LOSS)} = DCR \times I_L^2 = 0.003 \times (15 \text{ A})^2 = 675 \text{ mW}$$

Current Limit Programming

The valley current is approximately

$$15 \text{ A} - (5 \text{ A} \times 0.5) = 12.5 \text{ A}$$

Assuming a lower-side MOSFET R_{ON} of 4.5 mΩ, choosing 13 A as the valley current limit from Table 7 and Figure 71 indicates that a programming resistor (RES) of 100 kΩ corresponds to an A_{CS} of 24 V/V.

Choose a programmable resistor of R_{RES} = 100 kΩ for a current-sense gain of 24 V/V.

Output Capacitor

Assume a load step of 15 A occurs at the output, and no more than 5% is allowed for the output to deviate from the steady state operating point. Because the frequency is pseudo-fixed, the advantage of the ADP1882 is that the converter is able to respond quickly because of the immediate, though temporary, increase in switching frequency.

$$\Delta V_{DROOP} = 0.05 \times 1.8 \text{ V} = 90 \text{ mV}$$

Assuming the overall ESR of the output capacitor ranges from 5 mΩ to 10 mΩ,

$$C_{OUT} \quad 2 \times \frac{\Delta I_{LOAD}}{f_{SW} \quad (\Delta V_{DROOP})}$$

$$2 \times \frac{15 \text{ A}}{300 \quad 10^3 \times (90 \text{ mV})}$$

$$= 1.11 \text{ mF}$$

Therefore, an appropriate inductor selection is five 270 µF polymer capacitors with a combined ESR of 3.5 mΩ.

Assuming an overshoot of 45 mV, determine if the output capacitor that was calculated previously is adequate.

$$C_{OUT} = \frac{(L \times I^2_{LOAD})}{(V_{OUT} \quad V_{OVSHT})^2 - (V_{OUT})^2}$$

$$= \frac{1 \quad 10^{-6} \times (15 \text{ A})^2}{(1.8 \quad 45 \text{ mV})^2 - (1.8)^2}$$

$$= 1.4 \text{ mF}$$

Choose five 270 µF polymer capacitors.

The rms current through the output capacitor is

$$I_{RMS} \quad \frac{1}{2} \times \frac{1}{\sqrt{3}} \frac{(V_{IN,MAX} - V_{OUT})}{L \times f_{SW}} \times \frac{V_{OUT}}{V_{IN,MAX}}$$

$$\frac{1}{2} \times \frac{1}{\sqrt{3}} \frac{(13.2 \text{ V} - 1.8 \text{ V})}{1 \text{ µF} \quad 300 \times 10^3} \quad \frac{1.8 \text{ V}}{13.2 \text{ V}} = 1.49 \text{ A}$$

The power loss dissipated through the ESR of the output capacitor is

$$P_{COUT} = (I_{RMS})^2 \times ESR = (1.5 \text{ A})^2 \times 1.4 \text{ mΩ} = 3.15 \text{ mW}$$

Feedback Resistor Network Setup

It is recommended that R_B = 15 kΩ be used. Calculate R_T as follows:

$$R_T = 15 \text{ kΩ} \times \frac{(1.8 \text{ V} - 0.6 \text{ V})}{0.6 \text{ V}} = 30 \text{ kΩ}$$

Compensation Network

To calculate R_{COMP}, C_{COMP}, and C_{PAR}, the transconductance parameter and the current-sense gain variable are required. The transconductance parameter (G_M) is 500 µA/V, and the current-sense loop gain is

$$G_{CS} = \frac{1}{A_{CS} R_{ON}} = \frac{1}{26 \times 0.005} = 7.7 \text{ A/V}$$

where A_{CS} and R_{ON} are taken from setting up the current limit (see the Programming Resistor (RES) Detect Circuit and Valley Current-Limit Setting sections).

The crossover frequency is 1/12 of the switching frequency:

$$300 \text{ kHz}/12 = 25 \text{ kHz}$$

The zero frequency is 1/4 of the crossover frequency:

$$25 \text{ kHz}/4 = 6.25 \text{ kHz}$$

$$R_{COMP} = \frac{f_{CROSS}}{f_{CROSS} + f_{ZERO}} \times \frac{2\pi f_{CROSS} C_{OUT}}{G_M A_{CS}} \times \frac{V_{OUT}}{V_{REF}}$$

$$= \frac{25 \times 10^3}{25 \quad 10^3 \quad 6.25 \times 10^3} \times \frac{2 \quad 3.141 \quad 25 \quad 10^3 \quad 1.11 \times 10^{-3}}{500 \quad 10^{-6} \times 8.3} \times \frac{1.8}{0.8} = 75 \text{ kΩ}$$

$$C_{COMP} = \frac{1}{2\pi R_{COMP} f_{ZERO}}$$

$$= \frac{1}{2 \quad 3.14 \quad 75 \quad 10^3 \quad 6.25 \times 10^3}$$

$$= 340 \text{ pF}$$

Loss Calculations

Duty cycle = 1.8/12 V = 0.15.

$R_{ON\ (N2)}$ = 5.4 mΩ.

$t_{BODY(LOSS)}$ = 20 ns (body conduction time).

V_F = 0.84 V (MOSFET forward voltage).

C_{IN} = 3.3 nF (MOSFET gate input capacitance).

$Q_{N1,N2}$ = 17 nC (total MOSFET gate charge).

R_{GATE} = 1.5 Ω (MOSFET gate input resistance).

$$P_{N1,N2(CL)} = \left[D \times R_{N1(ON)} + (1 - D) \times R_{N2(ON)}\right] \times I_{LOAD}^2$$

= (0.15 × 0.0054 + 0.85 × 0.0054) × (15 A)²
= 1.215 W

$$P_{BODY(LOSS)} = \frac{t_{BODY(LOSS)}}{t_{SW}} \times I_{LOAD} \times V_F \times 2$$

= 20 ns × 300 × 10³ × 15 A × 0.84 × 2
= 151.2 mW

$P_{SW(LOSS)} = f_{SW} \times R_{GATE} \times C_{TOTAL} \times I_{LOAD} \times V_{IN} \times 2$
= 300 × 103 × 1.5 Ω × 3.3 × 10 − 9 × 15 A × 12 × 2
= 534.6 mW

$$P_{DR(LOSS)} = \left[V_{DR} \times \left(f_{SW} C_{upperFET} V_{DR} + I_{BIAS}\right)\right] + \left[V_{DD} \times \left(f_{SW} C_{upperFET} V_{DD} + I_{BIAS}\right)\right]$$

= (5.12 × (300 × 10³ × 3.3 × 10⁻⁹ × 5.12 + 0.002))
+ (5.5 × (300 × 10³ × 3.3 × 10⁻⁹ × 5.5 + 0.002))
= 77.13 mW

$P_{COUT} = (I_{RMS})^2 \times ESR$ = (1.5 A)² × 1.4 mΩ = 3.15 mW

$P_{DCR(LOSS)} = DCR \times I_{LOAD}^2$ = 0.003 × (15 A)² = 675 mW

$P_{CIN} = (I_{RMS})^2 \times ESR$ = (7.5 A)² × 1 mΩ = 56.25 mW

$P_{LOSS} = P_{N1,N2} + P_{BODY(LOSS)} + P_{SW} + P_{DCR} + P_{DR} + P_{COUT} + P_{CIN}$
= 1.215 W + 151.2 mW + 534.6 mW + 77.13 mW +
3.15 mW + 675 mW + 56.25 mW
= 2.62 W

EXTERNAL COMPONENT RECOMMENDATIONS

The configurations that are listed in Table 8 are with f_{CROSS} = 1/12 × f_{SW}, f_{ZERO} = ¼ × f_{CROSS}, R_{RES} = 100 kΩ, R_{BOT} = 15 kΩ, R_{ON} = 5.4 mΩ (BSC042N030MS G), V_{DD} = 5 V, and a maximum load current of 14 A. The ADP1883 models that are listed in Table 8 are the PSM versions of the device.

Table 8. External Component Values

	Marking Code										
SAP Model	ADP1882	ADP1883	V_{OUT} (V)	V_{IN} (V)	C_{IN} (µF)	C_{OUT} (µF)	L[1] (µH)	R_C (kΩ)	C_{COMP} (pF)	C_{PAR} (pF)	R_{TOP} (kΩ)
ADP1882ARMZ-0.3-R7/ ADP1883ARMZ-0.3-R7	LGF	LGJ	0.8	13	5 × 22[5]	5 × 560[2]	0.47	38.3	911	91	0.0
	LGF	LGJ	1.2	13	5 × 22[5]	4 × 560[2]	1.0	38.3	911	91	7.5
	LGF	LGJ	1.8	13	5 × 22[5]	5 × 270[3]	1.2	38.3	703	70	18.75
	LGF	LGJ	2.5	13	5 × 22[5]	3 × 270[3]	1.53	38.3	703	70	31.9
	LGF	LGJ	3.3	13	5 × 22[5]	3 × 330[4]	2.0	38.3	703	70	46.9
	LGF	LGJ	5	13	4 × 22[5]	330[4]	3.27	27.4	985	98	78.8
	LGF	LGJ	7	13	4 × 22[5]	22[5] + (4 × 47[6])	3.44	27.4	985	98	116.3
	LGF	LGJ	1.2	16.5	5 × 22[5]	4 × 560[2]	1.0	38.3	911	91	7.5
	LGF	LGJ	1.8	16.5	4 × 22[5]	4 × 270[3]	1.0	38.3	729	73	18.8
	LGF	LGJ	2.5	16.5	4 × 22[5]	4 × 270[3]	1.67	38.3	729	73	31.9
	LGF	LGJ	3.3	16.5	4 × 22[5]	3 × 330[4]	2.00	38.3	729	73	46.9
	LGF	LGJ	5	16.5	3 × 22[5]	2 × 150[7]	3.84	27.4	1020	102	78.8
	LGF	LGJ	7	16.5	3 × 22[5]	22[5] + 4 × 47[6]	4.44	27.4	1020	102	116.3
ADP1882ARMZ-0.6-R7/ ADP1883ARMZ-0.6-R7	LGG	LGK	0.8	5.5	5 × 22[5]	4 × 560[2]	0.22	38.3	418	42	0.0
	LGG	LGK	1.2	5.5	5 × 22[5]	4 × 270[3]	0.47	38.3	401	40	7.5
	LGG	LGK	1.8	5.5	5 × 22[5]	3 × 270[3]	0.47	38.3	334	33	18.8
	LGG	LGK	2.5	5.5	5 × 22[5]	3 × 180[8]	0.47	38.3	334	33	31.9
	LGG	LGK	1.2	13	5× 22[5]	5 × 270[3]	0.47	38.3	501	50	7.5
	LGG	LGK	1.8	13	5 × 10[9]	3 × 330[4]	0.72	38.3	378	38	18.8
	LGG	LGK	2.5	13	5 × 10[9]	3 × 270[3]	0.90	38.3	378	38	31.9
	LGG	LGK	3.3	13	5 × 10[9]	2 × 270[3]	1.00	38.3	378	38	46.9
	LGG	LGK	5	13	5 × 10[9]	150[7]	1.76	27.4	529	53	78.8
	LGG	LGK	1.2	16.5	3 × 10[9]	4 × 270[3]	0.47	38.3	445	45	7.5
	LGG	LGK	1.8	16.5	4 × 10[9]	2 × 330[4]	0.72	38.3	401	40	18.8
	LGG	LGK	2.5	16.5	4 × 10[9]	3 × 270[3]	0.90	38.3	401	40	31.9
	LGG	LGK	3.3	16.5	4 × 10[9]	330[4]	1.0	38.3	364	36	46.9
	LGG	LGK	5	16.5	4 × 10[9]	4 × 47[6]	2.0	27.4	510	51	78.8
	LGG	LGK	7	16.5	4 × 10[9]	3 × 47[6]	2.0	27.4	468	47	116.3
ADP1882ARMZ-1.0-R7/ ADP1883ARMZ-1.0-R7	LGH	LGL	0.8	5.5	5 × 22[5]	4 × 270[3]	0.22	38.3	275	27	0.0
	LGH	LGL	1.2	5.5	5 × 22[5]	2 × 330[4]	0.22	38.3	275	27	7.5
	LGH	LGL	1.8	5.5	3 × 22[5]	3 × 180[8]	0.22	38.3	200	20	18.8
	LGH	LGL	2.5	5.5	3 × 22[5]	270[3]	0.22	38.3	200	20	31.9
	LGH	LGL	1.2	13	4 × 10[9]	3 × 330[4]	0.22	38.3	286	29	7.5
	LGH	LGL	1.8	13	4 × 10[9]	3 × 270[3]	0.47	38.3	259	26	18.8
	LGH	LGL	2.5	13	4 × 10[9]	2 x 270[3]	0.47	38.3	259	26	31.9
	LGH	LGL	3.3	13	5 × 10[9]	270[3]	0.72	38.3	259	26	46.9
	LGH	LGL	5	13	4 × 10[9]	3 × 47[6]	1.0	27.4	330	33	78.8
	LGH	LGL	1.2	16.5	4 × 10[9]	4 × 270[3]	0.47	38.3	401	40	7.5
	LGH	LGL	1.8	16.5	4 × 10[9]	3 × 270[3]	0.47	38.3	321	32	18.8
	LGH	LGL	2.5	16.5	4 × 10[9]	3 × 180[8]	0.72	38.3	286	29	31.9
	LGH	LGL	3.3	16.5	4 × 10[9]	270[3]	0.72	38.3	267	27	46.9

SAP Model	Marking Code		V_{OUT} (V)	V_{IN} (V)	C_{IN} (µF)	C_{OUT} (µF)	L[1] (µH)	R_C (kΩ)	C_{COMP} (pF)	C_{PAR} (pF)	R_{TOP} (kΩ)
	ADP1882	ADP1883									
	LGH	LGL	5	16.5	3 × 10[9]	3 × 47[6]	1.4	27.4	330	33	78.8
	LGH	LGL	7	16.5	3 × 10[9]	22[5] + 47[6]	1.4	27.4	281	28	116.3

[1] See the Inductor Selection section (see Table 9).
[2] 560 µF Panasonic (SP-series) 2 V, 7 mΩ, 3.7 A EEFUE0D561LR (4.3 mm × 7.3 mm × 4.2 mm).
[3] 270 µF Panasonic (SP-series) 4 V, 7 mΩ, 3.7 A EEFUE0G271LR (4.3 mm × 7.3 mm × 4.2 mm).
[4] 330 µF Panasonic (SP-series) 4 V, 12 mΩ, 3.3 A EEFUE0G331R (4.3 mm × 7.3 mm × 4.2 mm).
[5] 22 µF Murata 25 V, X7R, 1210 GRM32ER71E226KE15L (3.2 mm × 2.5 mm × 2.5 mm).
[6] 47 µF Murata 16 V, X5R, 1210 GRM32ER61C476KE15L (3.2 mm × 2.5 mm × 2.5 mm).
[7] 150 µF Panasonic (SP-series) 6.3 V, 10 mΩ, 3.5 A EEFUE0J151XR (4.3 mm × 7.3 mm × 4.2 mm).
[8] 180 µF Panasonic (SP-series) 4 V, 10 mΩ, 3.5 A EEFUE0G181XR (4.3 mm × 7.3 mm × 4.2 mm).
[9] 10 µF TDK 25 V, X7R, 1210 C3225X7R1E106M.

Table 9. Recommended Inductors

L (µH)	DCR (mΩ)	I_{SAT} (A)	Dimension (mm)	Manufacturer	Model Number
0.12	0.33	55	10.2 × 7	Wurth Electronics	744303012
0.22	0.33	30	10.2 × 7	Wurth Electronics	744303022
0.47	0.8	50	14.2 × 12.8	Wurth Electronics	744355147
0.72	1.65	35	10.5 × 10.2	Wurth Electronics	744325072
0.9	1.6	28	13 × 12.8	Wurth Electronics	744355090
1.2	1.8	25	10.5 × 10.2	Wurth Electronics	744325120
1.0	3.3	20	10.5 × 10.2	Wurth Electronics	7443552100
1.4	3.2	24	14 × 12.8	Wurth Electronics	744318180
2.0	2.6	22	13.2 × 12.8	Wurth Electronics	7443551200
0.8		27.5		Sumida	CEP125U-0R8

Table 10. Recommended MOSFETs

V_{GS} = 4.5 V	R_{ON} (mΩ)	I_D (A)	V_{DS} (V)	C_{IN} (nF)	Q_{TOTAL} (nC)	Package	Manufacturer	Model Number
Upper-Side MOSFET (Q1/Q2)	5.4	47	30	3.2	20	PG-TDSON8	Infineon	BSC042N03MS G
	10.2	53	30	1.6	10	PG-TDSON8	Infineon	BSC080N03MS G
	6.0	19	30		35	SO-8	Vishay	Si4842DY
	9	14	30	2.4	25	SO-8	International Rectifier	IRF7811
Lower-Side MOSFET (Q3/Q4)	5.4	47	30	3.2	20	PG-TDSON8	Infineon	BSC042N030MS G
	10.2	82	30	1.6	10	PG-TDSON8	Infineon	BSC080N030MS G
	6.0	19	30		35	SO-8	Vishay	Si4842DY

LAYOUT CONSIDERATIONS

The performance of a dc-to-dc converter depends highly on how the voltage and current paths are configured on the printed circuit board (PCB). Optimizing the placement of sensitive analog and power components are essential to minimize output ripple, maintain tight regulation specifications, and reduce PWM jitter and electromagnetic interference.

Figure 83 shows the schematic of a typical ADP1882/ADP1883 used for a high power application. Blue traces denote high current pathways. VIN, PGND, and V_{OUT} traces should be wide and possibly replicated, descending down into the multiple layers. Vias should populate, mainly around the positive and negative terminals of the input and output capacitors, alongside the source of Q1/Q2, the drain of Q3/Q4, and the inductor.

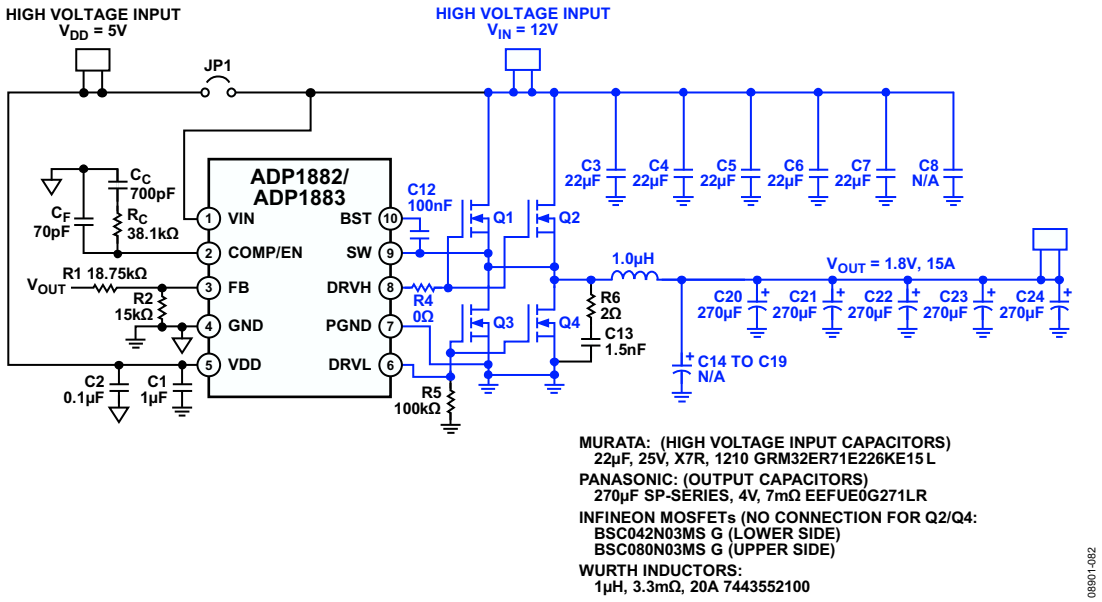

Figure 83. ADP1882 High Current Evaluation Board Schematic (Blue Traces Indicate High Current Paths)

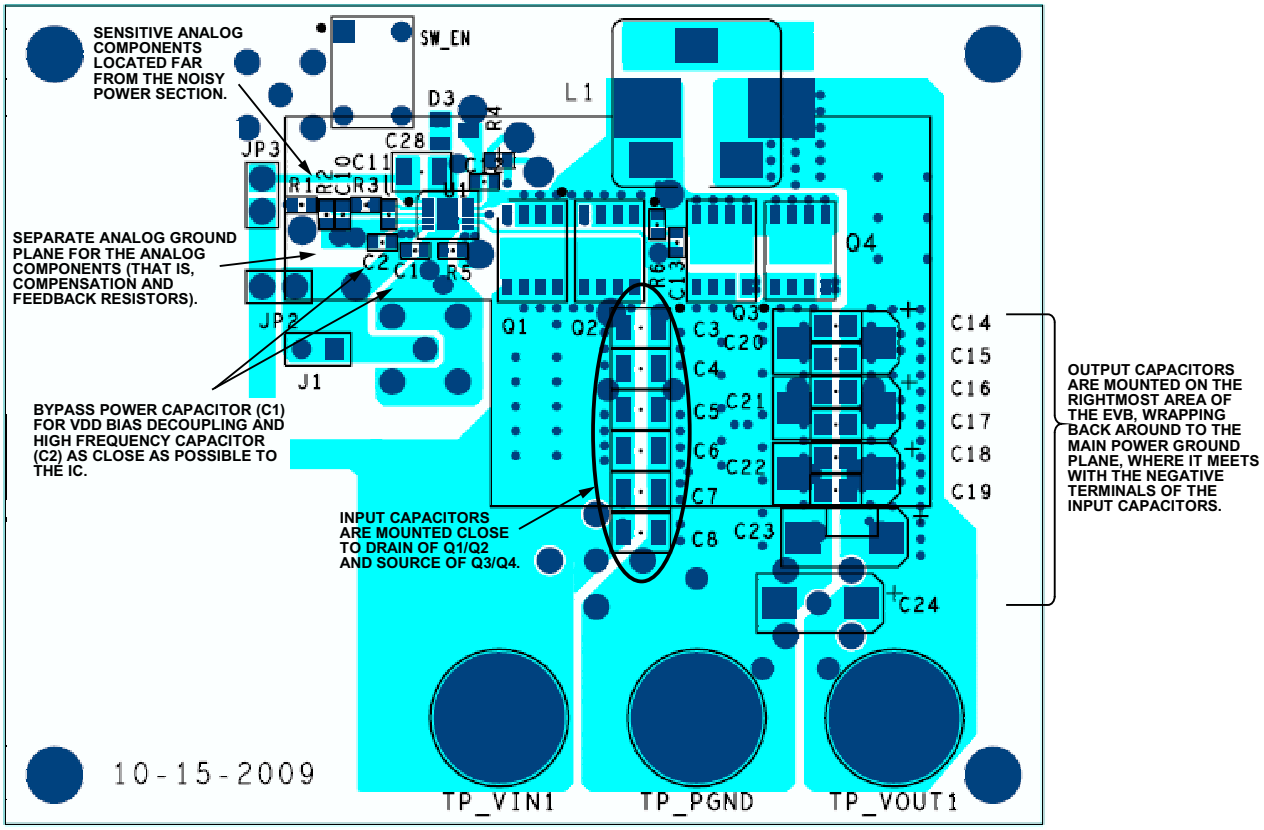

Figure 84. Overall Layout of the ADP1882 High Current Evaluation Board

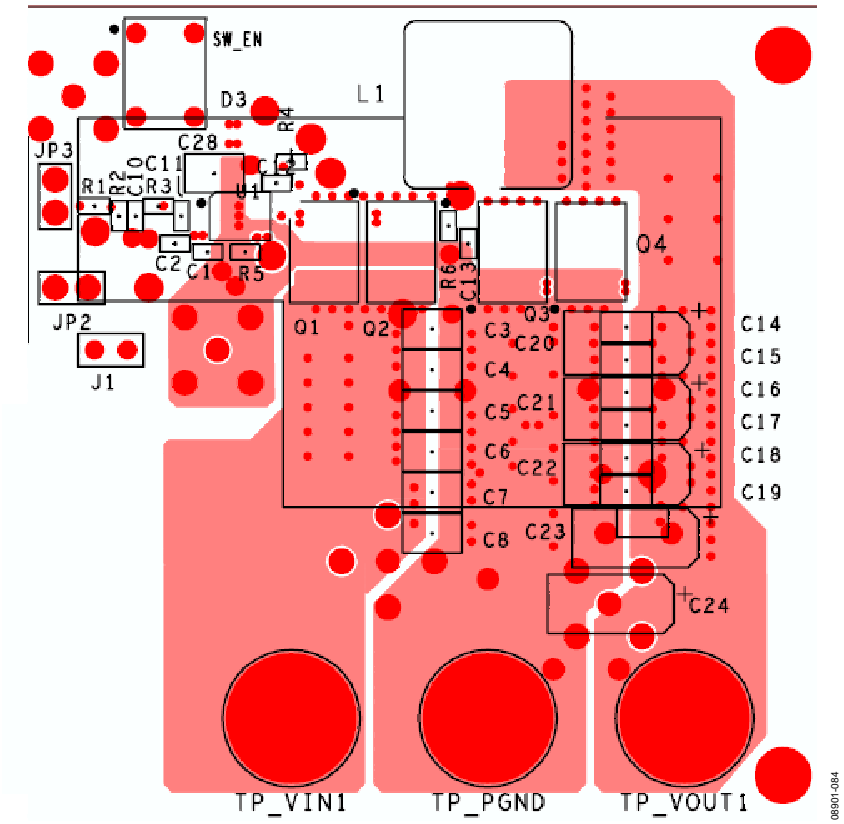

Figure 85. Layer 2 of Evaluation Board

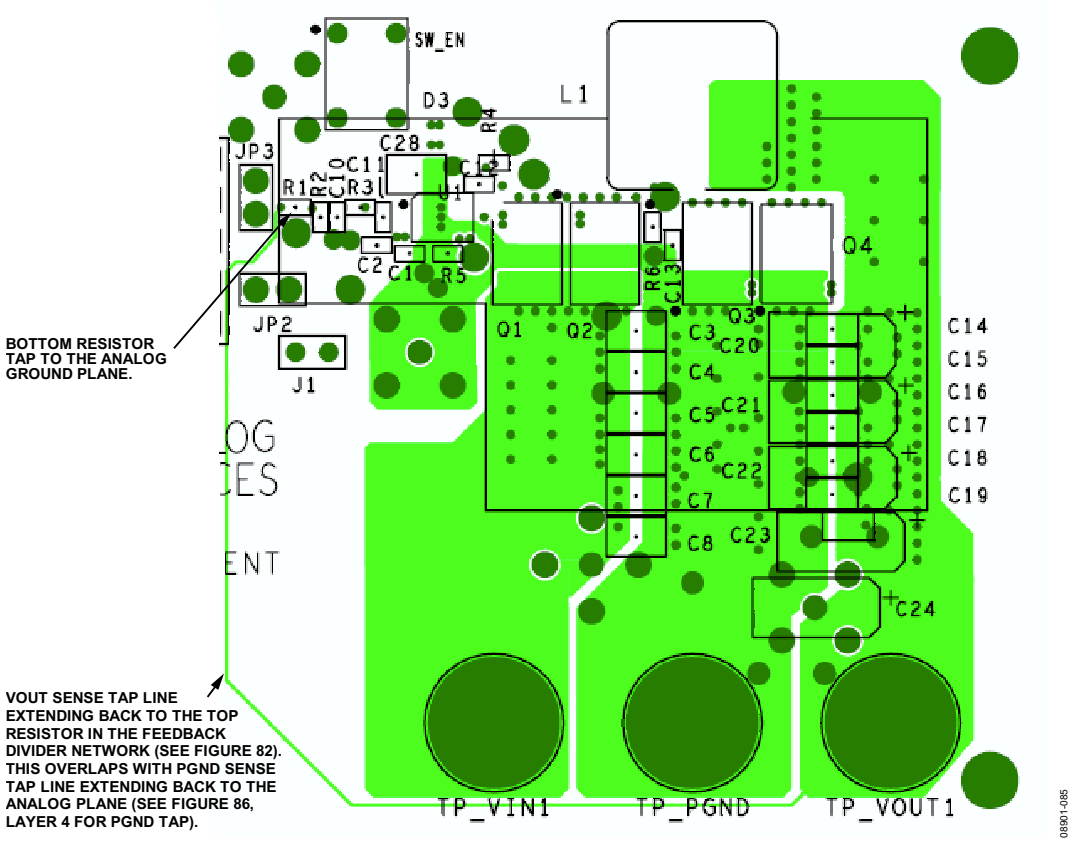

Figure 86. Layer 3 of Evaluation Board

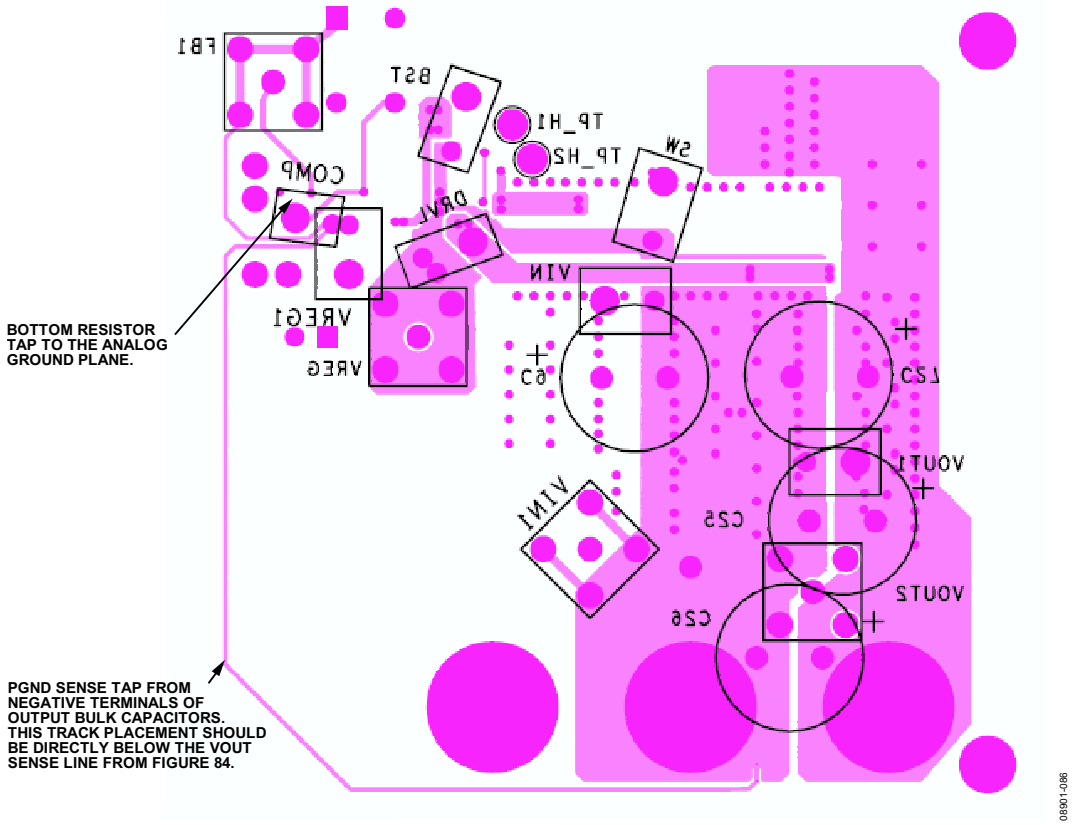

Figure 87. Layer 4 (Bottom Layer) of Evaluation Board

IC SECTION (LEFT SIDE OF EVALUATION BOARD)

A dedicated plane for the analog ground plane (GND) should be separate from the main power ground plane (PGND). With the shortest path possible, connect the analog ground plane to the GND pin (Pin 4). This plane should be on only the top layer of the evaluation board. To avoid crosstalk interference, there should not be any other voltage or current pathway directly below this plane on Layer 2, Layer 3, or Layer 4. Connect the negative terminals of all sensitive analog components to the analog ground plane. Examples of such sensitive analog components include the bottom resistor of the resistor divider, the high frequency bypass capacitor for biasing (0.1 µF), and the compensation network.

Mount a 1 µF bypass capacitor directly across VDD (Pin 5) and PGND (Pin 7). In addition, a 0.1 µF should be tied across VDD (Pin 5) and GND (Pin 4).

POWER SECTION

As shown in Figure 84, an appropriate configuration to localize large current transfer from the high voltage input (V_{IN}) to the output (V_{OUT}), and then back to the power ground, puts the V_{IN} plane on the left, the output plane on the right, and the main power ground plane in between the two. Current transfers from the input capacitors to the output capacitors, through Q1/Q2, during the on state (see Figure 88). The direction of this current (yellow arrow) is maintained as Q1/Q2 turns off and Q3/Q4 turns on. When Q3/Q4 turns on, the current direction continues to be maintained (red arrow) as it circles from the power ground terminal of the bulk capacitor to the output capacitors, through the Q3/Q4. Arranging the power planes in this manner minimizes the area in which changes in flux occur if the current through Q1/Q2 stops abruptly. Sudden changes in flux, usually at the source terminals of Q1/Q2 and the drain terminals of Q3/Q4, cause large dV/dt's at the SW node.

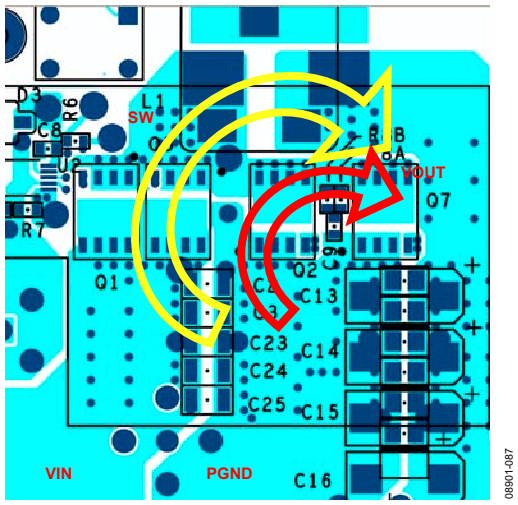

Figure 88. Primary Current Pathways During the On State of the Upper-Side MOSFET (Left Arrow) and the On State of the Lower-Side MOSFET (Right Arrow)

The SW node is near the top of the evaluation board. The SW node should use the least amount of area possible and be kept away from any sensitive analog circuitry and components because this is where most sudden changes in flux density occur. When possible, replicate this pad onto Layer 2 and Layer 3 for thermal relief and eliminate any other voltage and current pathways directly beneath the SW node plane. Populate the SW node plane with vias, mainly around the exposed pad of the inductor terminal and around the perimeter of the source of Q1/Q2 and the drain of Q3/Q4. The output voltage power plane (V_{OUT}) is at the rightmost end of the evaluation board. This plane should be replicated, descending down to multiple layers with vias surrounding the inductor terminal and the positive terminals of the output bulk capacitors. Ensure that the negative terminals of the output capacitors are placed close to the main power ground (PGND), as previously mentioned. All of these points form a tight circle (component geometry permitting) that minimizes the area of flux change as the event switches between D and 1 − D.

DIFFERENTIAL SENSING

Because the ADP1882/ADP1883 operate in valley current-mode control, a differential voltage reading is taken across the drain and source of the lower-side MOSFET. The drain of the lower-side MOSFET should be connected as close as possible to Pin 9 (SW) of the IC. Likewise, connect the source as close as possible to Pin 7 (PGND) of the IC. When possible, both of these track lines should be narrow and away from any other active device or voltage/current paths.

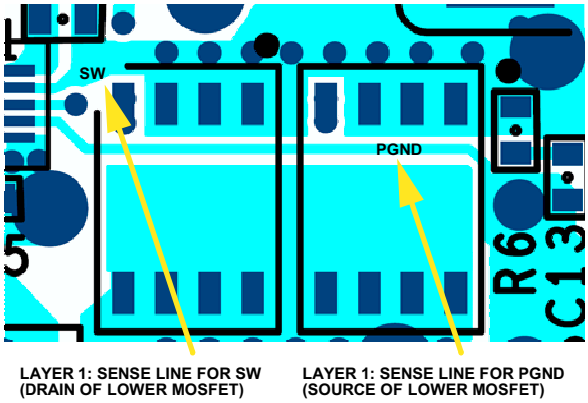

Figure 89. Drain/Source Tracking Tapping of the Lower-Side MOSFET for CS Amp Differential Sensing (Yellow Sense Line on Layer 2)

Differential sensing should also be applied between the outermost output capacitor to the feedback resistor divider (see Figure 86 and Figure 87). Connect the positive terminal of the output capacitor to the top resistor (R_T). Connect the negative terminal of the output capacitor to the negative terminal of the bottom resistor, which connects to the analog ground plane, as well. Both of these track lines, as previously mentioned, should be narrow and away from any other active device or voltage/current paths.

TYPICAL APPLICATIONS CIRCUITS

DUAL-INPUT, 300 kHz HIGH CURRENT APPLICATIONS CIRCUIT

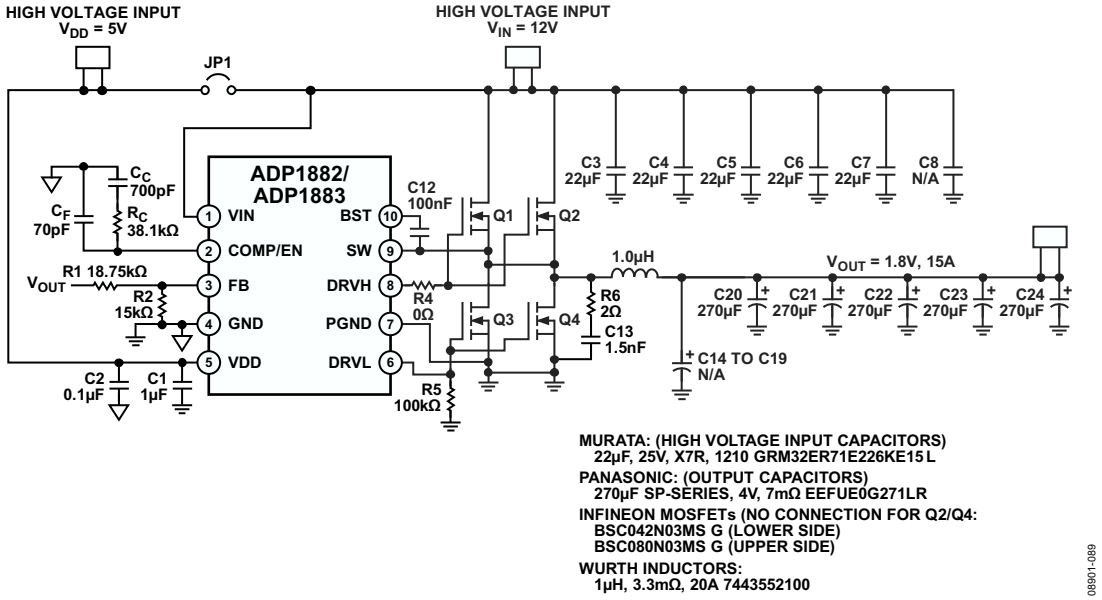

Figure 90. Applications Circuit for 12 V Input, 1.8 V Output, 15 A, 300 kHz (Q2/Q4 No Connect)

SINGLE-INPUT, 600 kHz APPLICATIONS CIRCUIT

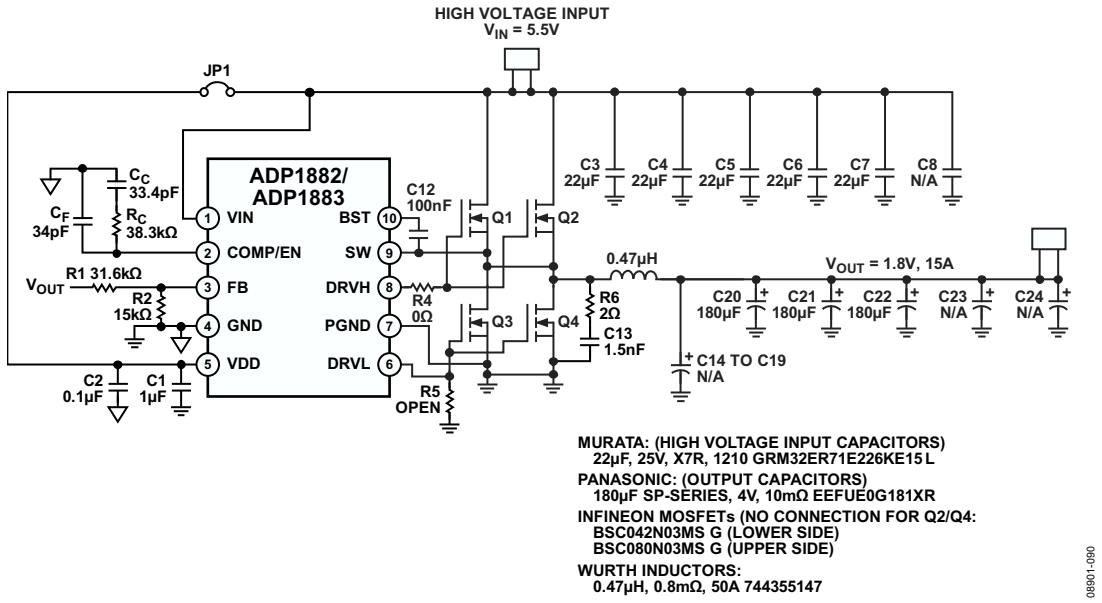

Figure 91. Applications Circuit for 5.5 V Input, 2.5 V Output, 15 A, 600 kHz (Q2/Q4 No Connect)

DUAL-INPUT, 300 kHz HIGH CURRENT APPLICATIONS CIRCUIT

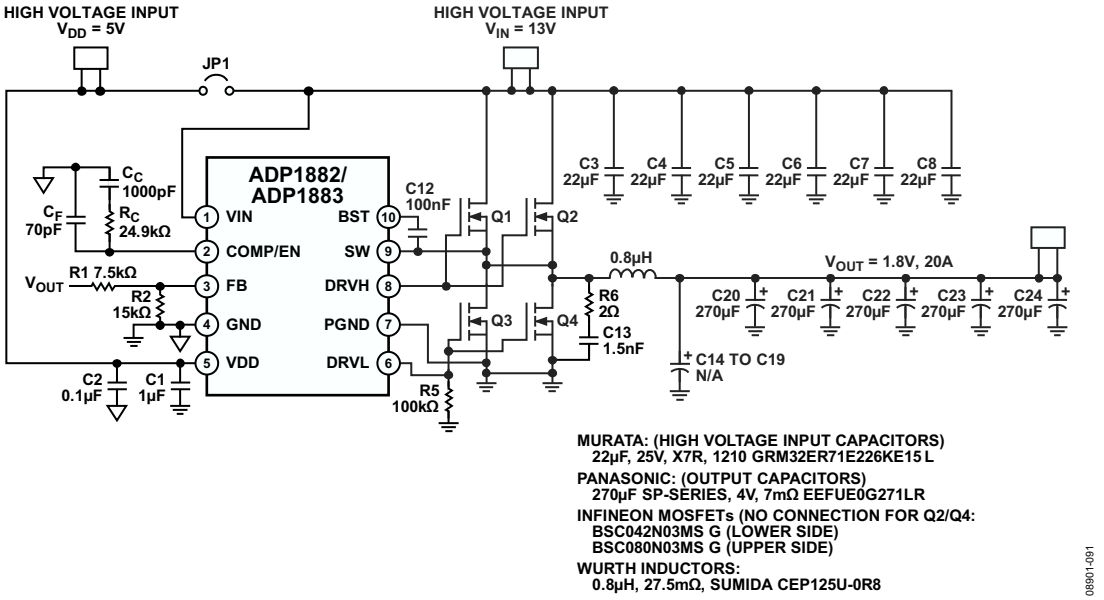

Figure 92. Applications Circuit for 13 V Input, 1.8 V Output, 20 A, 300 kHz (Q2/Q4 No Connect)

OUTLINE DIMENSIONS

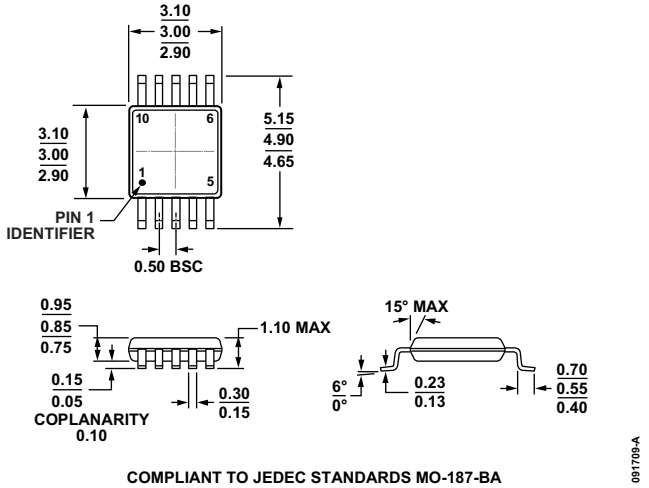

Figure 93. 10-Lead Mini Small Outline Package [MSOP]
(RM-10)
Dimensions shown in millimeters

ORDERING GUIDE

Model[1]	Temperature Range	Package Description	Package Option	Branding
ADP1882ARMZ-0.3-R7	−40°C to +125°C	10-Lead Mini Small Outline Package [MSOP]	RM-10	LGF
ADP1882ARMZ-0.6-R7	−40°C to +125°C	10-Lead Mini Small Outline Package [MSOP]	RM-10	LGG
ADP1882ARMZ-1.0-R7	−40°C to +125°C	10-Lead Mini Small Outline Package [MSOP]	RM-10	LGH
ADP1882ARMZ-0.3-EVALZ		Forced PWM, 300 kHz Evaluation Board		
ADP1882ARMZ-0.6-EVALZ		Forced PWM, 600 kHz Evaluation Board		
ADP1882ARMZ-1.0-EVALZ		Forced PWM, 1.0 MHz Evaluation Board		
ADP1883ARMZ-0.3-R7	−40°C to +125°C	10-Lead Mini Small Outline Package [MSOP]	RM-10	LGJ
ADP1883ARMZ-0.6-R7	−40°C to +125°C	10-Lead Mini Small Outline Package [MSOP]	RM-10	LGK
ADP1883ARMZ-1.0-R7	−40°C to +125°C	10-Lead Mini Small Outline Package [MSOP]	RM-10	LGL
ADP1883ARMZ-0.3-EVALZ		Power Saving Mode, 300 kHz Evaluation Board		
ADP1883ARMZ-0.6-EVALZ		Power Saving Mode, 600 kHz Evaluation Board		
ADP1883ARMZ-1.0-EVALZ		Power Saving Mode, 1.0 MHz Evaluation Board		

[1] Z = RoHS Compliant Part.

NOTES

D08901-0-4/10(0)